



ELSEVIER

Contents lists available at ScienceDirect

SLAS Technology

journal homepage: www.elsevier.com/locate/slast

Full Length Article

Recent progress of 4D printing in cancer therapeutics studies

Atchara Chinnakorn^a, Wiwat Nuansing^a, Mahdi Bodaghi^b, Bernard Rolfe^c, Ali Zolfagharian^{c,*}^a School of Physics, Institute of Science, Suranaree University of Technology, Nakhon Ratchasima 30000, Thailand^b Department of Engineering, School of Science and Technology, Nottingham Trent University, Nottingham NG11 8NS, United Kingdom^c School of Engineering, Deakin University, Geelong, Victoria 3216, Australia

ARTICLE INFO

Keywords:

4D printing
Cancer therapeutics
Surgical resection
Drug delivery system
Hyperthermia

ABSTRACT

Cancer is a critical cause of global human death. Not only are complex approaches to cancer prognosis, accurate diagnosis, and efficient therapeutics concerned, but post-treatments like postsurgical or chemotherapeutic effects are also followed up. The four-dimensional (4D) printing technique has gained attention for its potential applications in cancer therapeutics. It is the next generation of the three-dimensional (3D) printing technique, which facilitates the advanced fabrication of dynamic constructs like programmable shapes, controllable locomotion, and on-demand functions. As is well-known, it is still in the initial stage of cancer applications and requires the insight study of 4D printing. Herein, we present the first effort to report on 4D printing technology in cancer therapeutics. This review will illustrate the mechanisms used to induce the dynamic constructs of 4D printing in cancer management. The recent potential applications of 4D printing in cancer therapeutics will be further detailed, and future perspectives and conclusions will finally be proposed.

Introduction

Additive manufacturing (AM) or three-dimensional (3D) printing technology which builds up the successively layer-by-layer manner of materials, has attracted attention in a wide range of applications because there are various alternatives of materials in the manufacturing process, accessible adaptabilities in the process, as well as its ability to easily produce intricate objects [1–3]. 3D printing has been further

advanced with the addition of a fourth dimension, resulting in the concept of four-dimensional (4D) printing. 4D printing technology is an advanced fabrication of dynamic products which can respond to specific stimuli such as light, temperature, magnetic field, electrical field, ultrasound, pH value, enzymes, and so on [4]. It applies smart materials to the fabrication procedure of the existing 3D printing technology [4,5]. Smart materials allow changes in the printed constructs over time by following specific stimuli [6,7]. Their stimuli-responsive behaviors

Abbreviations: AI, artificial intelligence; Alg, alginate; AM, additive manufacturing; AMF, alternating magnetic field; AUD, aliphatic urethane diacrylate; AuNPs, gold nanoparticles; AuNRs, gold nanorods; BPADMA, bisphenol A ethoxylate dimethacrylate; ChMA, methacrylamide chitosan; CRC, corrector cancer; Cy-7, Cyanine7; DDSs, drug delivery systems; DEGDA, di(ethylene glycol) diacrylate; DEX, dexamethasone; DIW, direct ink writing; DLP, digital light processing; DOX, doxorubicin; DOX-HCl, doxorubicin hydrochloride; EVA, ethylene-vinyl acetate; FDM, fused deposition modeling; FFF, fused filament fabrication; FLU, 5-fluorouracil; Fs-DLW, femto-second direct laser writing; Gel, gelatin; GelMA, gelatin methacryloyl; GO, graphene oxide; HAase, hyaluronidase; hIn, human insulin; IBOA, isobornyl acrylate; IONs, iron oxide nanoparticles; LA, lauric acid; L-PBF, laser powder bed fusion; MC, methylcellulose; Mel, melanin; ML, machine learning; MMPs, matrix metalloproteinases; MNPs, magnetic nanoparticles; MTX, methotrexate; M-PSL, magnetic field-assisted projection stereolithography; NIR, near-infrared; OS, osteosarcoma; SA, stearic acid; SA-MA, methacrylated alginate; SEM, scanning electron microscope; SLA, stereolithography; SMAs, shape memory alloys; SME, shape memory effect; SMPs, shape memory polymers; SPIONs, superparamagnetic iron oxide nanoparticles; PAA, polyacrylic acid; PAAM, polyacrylamide; PBS, phosphate-buffered saline; PCL, poly(ϵ -caprolactone), polycaprolactone; PCLDA, poly(ϵ -caprolactone)-diacrylates; PDMS, polydimethylsiloxane; PEGDA, poly(ethylene glycol) diacrylate; PEO-PPO-PEO, poly(ethylene oxide)-*b*-poly(propylene oxide)-*b*-poly(ethylene oxide); PGDA, poly(glycerol dodecanoate) acrylate; PGMEA, propylene glycol methyl ether acetate; PLA, poly(lactic acid); PLGA, poly(lactic-co-glycolic acid); PTX, paclitaxel; poly(DLLA-co-CL)MA, poly(D,L-lactide-co- ϵ -caprolactone) methacrylate; PVP, polyvinylpyrrolidone; PU, poly(ether urethane); P μ SL, projection microstereolithography; P(DLLA-TMC), poly(lactic acid-co-trimethylene carbonate); tBA, tert-Butyl acrylate; TCP, β -tricalcium phosphate; T_m, melting temperature; T_g, glass transition temperature; T_{trans}, transition temperature; TDLW, two-photon direct laser writing; UV, ultraviolet; 3D, three-dimensional; 4D, four-dimensional.

* Corresponding author.

E-mail address: a.zolfagharian@deakin.edu.au (A. Zolfagharian).<https://doi.org/10.1016/j.slast.2023.02.002>

Received 28 December 2022; Received in revised form 7 February 2023; Accepted 13 February 2023

Available online xxx

2472-6303/© 2023 The Authors. Published by Elsevier Inc. on behalf of Society for Laboratory Automation and Screening. This is an open access article under the CC BY-NC-ND license (<http://creativecommons.org/licenses/by-nc-nd/4.0/>)Please cite this article as: A. Chinnakorn, W. Nuansing, M. Bodaghi et al., Recent progress of 4D printing in cancer therapeutics studies, SLAS Technology, <https://doi.org/10.1016/j.slast.2023.02.002>

have been considered another dimension of the manufacturing procedure. It can be mentioned that time is the 4th dimension of the process [3,8-10]. Although 3D printing technology has manifested in wide medical applications with the advantages of precisely defined architecture and individual constructs [8,11-14], there are still challenges, such as scalability and static structures that cannot change over time or adapt to dynamic environments [8,15]. Thus, 4D printing has emerged to address these challenges and play a significant role in the innovative fabrication of dynamic constructs.

Cancer is a severe health problem that results in morbidity and mortality. Cancer death has been considered one in six global deaths [16], the second cause of death worldwide [17-19]. In addition, there is still an increasing trend in the future, with 13.1 million cases expected in 2030 [19,20]. With the complexity of cancer disease and patient heterogeneity, one-size-fits-all treatments could not provide satisfactory outcomes [12]. Although cancer is a severe issue, it can be curable if there are accurate diagnoses and effective treatments in the early stages, such as colorectal cancer [21]. Compared with normal tissues, cancer and tumor tissues have particular environments because of abnormal metabolisms [7,22]. In particular, enzymes such as protease (like matrix metalloproteinases (MMPs)), esterase, hyaluronidase (HAase), and so on present upregulated levels in cancer and tumor regions [7,22]. Besides, the pH of the regions is more acidic than regular sites such as intracellular endosomes (pH = 5.0-6.5) and extracellular sites (pH = 6.5-7.2) because the high glycolysis rate of cancer provides overproduction and secretion of lactic acid [7,23]. These factors can be used as biomarkers that identify the targeted cancer area [24,25]. Therefore, the incorporation of smart materials, such as pH- or enzyme-responsive materials, in 4D printing has the potential to enhance localized treatments owing to the specific microenvironment of cancer. In addition, other types of smart materials, including light-responsive, magneto-responsive, and temperature-responsive materials have the potential to play crucial roles in creating dynamic constructs for 4D printing applications [26-28]. The utilization of smart materials in 4D printing for cancer therapeutics will be illustrated in this review article.

As mentioned, 4D printing has intervened to enhance the potential of cancer therapeutics such as operation, hyperthermia, photothermal therapy, chemotherapy, and therapeutic devices. Therefore, it is possibly anticipated as the next alternative to cancer management, which offers potentially personalized treatments. Recently, there has been a review of 3D and 4D printing in the fight against breast cancer, the second most common cancer in the world [29]. It has been pointed out that the advanced potential of breast cancer management with 3D and 4D printings has allowed new strategies to achieve on-demand management. Since 4D printing is still in its early stages, it requires an understanding of materials and a demonstration of application possibilities. This article is the first overview of 4D printing applications in cancer therapeutics, to the best of authors' knowledge (see Fig. 1). This overview will first be presented through 4D printing approaches like a shape memory effect (SME), magnetothermal and magnetically-driven effects, a photothermal effect, swelling and shrinking effects, and a biologically-driven effect. Then, the point of how the effects apply to 4D printing in potential applications in cancer therapeutics will be illustrated. Finally, challenges and future perspectives will be proposed.

Mechanisms of 4D printing approaches

4D printing utilizes smart materials in the manufacturing procedure of existing 3D printing. Smart materials refer to materials that enable response to specific stimuli, leading to changes like shape transformation, controllable functions, and property changes [4,30]. Recent publications summarized categories of smart materials in the field of medical applications as physical, chemical, biological, and multi-stimuli, [6,8,30] which are used to perform the change of dynamic constructs. Herein, we present the mechanisms of 4D printing approaches, which are included in Table 1 and illustrated in Fig. 2: SME, magnetothermal

and magnetic driving effects, photothermal effects, swelling and shrinking effects, and biologically-driven effects. The details of potential applications in cancer treatments will be illustrated in the next section.

Shape memory effect (SME)

The SME is a performance in which materials can remember their shape. They enable geometry to recover to the original shape (one-way change) or change reversible shape changes (two-way or multiple-way changes) [55] under stimuli such as heat, light, humidity, pH, electricity, or magnetic field [56]. It can minimize the volume of biomedical devices, scaffolds, or implants inserted into the body, which eases incisions and patients' injuries [39]. For example, Kim and Lee [31] fabricated bifurcated stents based on shape memory polyurethane (PU), and the stents with a kirigami structure smoothly traveled inside a mocked vessel with branched parts. The SME has appeared in several materials, such as alloys, polymers, hydrogels, and composites, induced by various phase transformations.

Shape memory alloys (SMA) such as Au-Cd, Cu-Sn, Ti-Pd, Ni-Al, Ni-Al, Cu-Zn-Al, Fe-Mn-Si, Ni-Ti-Cu, nitinol, or an equiatomic nickel and titanium alloy [5,57] have been performed through martensitic transformation, which can be triggered with temperature or high mechanical load. The SME of alloys is carried out under the change of twinned and detwinned martensite [5,58]. For instance, Kim, Ferretto, Leinenbach and Lee [32] fabricated complex structures of Fe-based SMA (Fe-SMA). The Fe-17Mn-5Si-10Cr-4Ni (wt.%) powder was chosen in a fabrication process with laser powder bed fusion (L-PBF). The Fe-SMA-based strip was easily deformed by bending without damage, and the bent strip could completely recover within 5 s when heated at 300°C, as shown in Fig. 2(a). Moreover, the Fe-SMA-based metamaterial presented a self-healing behavior.

Shape memory polymers (SMPs) such as poly(lactic acid) (PLA)[33,40], PU [38,59], polycaprolactone triol, poly(ϵ -caprolactone) dimethacrylate[8] can perform a change when shifted between the glass state and rubber state[9]. Their SME employs a transition temperature (T_{trans}) which is a melting temperature (T_m) for semicrystalline polymers and a glass transition temperature (T_g) for amorphous polymers [58,60]. The SME has four stages that are: (1) a printed object is heated up to a constant temperature that is higher than T_g , (2) the object is loaded, and its shape is transformed to the desired one, (3) the loaded object is cooled down to a lower temperature that is lower than T_g , and the mechanical constraints are removed while an inelastic strain is in the object, resulting in a programmed shape, (4) the object is reheated to obtain the original shape [15]. For example, Jia, Gu and Chang [33] presented a self-expandable vascular stent based on shape memory PLA, an intelligent solution for stent implantation in cardiovascular disease. The stent with a hexagonal nested structure was fabricated by a fused deposition modeling (FDM) 3D printer. The printed stent was deformed to a temporary shape by compression at 70°C. Amorphous PLA chains served as the switchable components, which achieved external response and memorized temporary shape. The compressed stent maintained the temporary shape for over a week at room temperature. The temporary shape rapidly recovered to the original shape within 5 s at 70°C. The temperature used to induce the SMP in implantation applications has introduced that it should be in a range of 20°C to 37°C to prevent harm to the body [58]. Pandey, Mohol and Kandi [34] modified the shape and functionality of a PLA/poly(ϵ -caprolactone) (PCL) composite. PLA served as a fixed phase to memorize an original shape, and PCL acted as a reversible phase to modify the transition and fixation of a temporary shape. The T_{trans} of PLA/PCL blends decreased with the increase of PCL from 61.5°C to 49.1°C for a ratio of PLA30/PCL70; however, the decrease of PLA content decreased the recovery ratio from 97% to 73%, as seen in Fig. 2(b). PLA70/PCL30 provided the optimum fixity and recovery ratio. The PLA70/PCL30 tracheal scaffolds showed shape memory performance in hot water. The tracheal scaffolds received the original shape and fitted to the

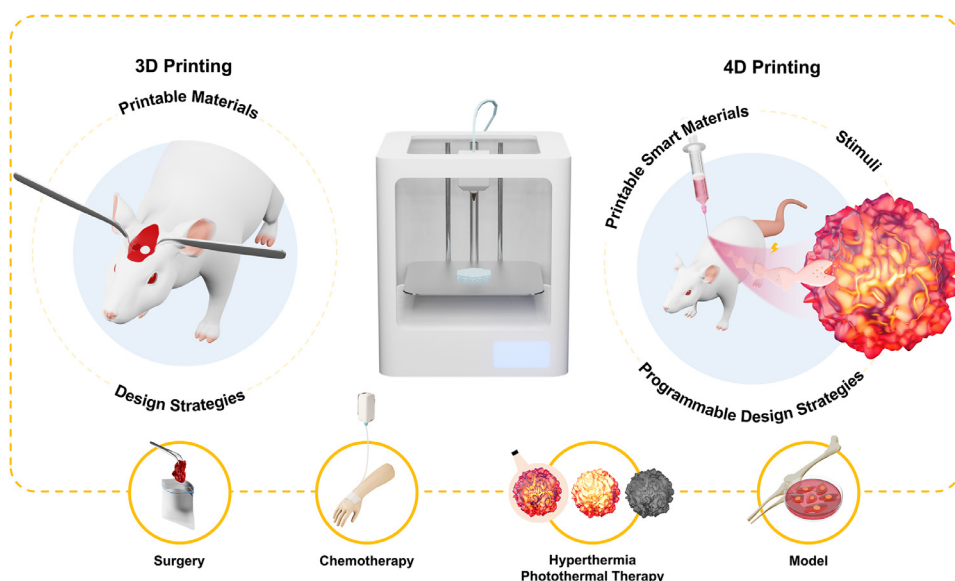


Fig. 1. Shows schematic illustration of 3D and 4D printing technologies in advanced applications of cancer management.

Table 1

The conclusive effects including shape memory, magnetothermal/ magnetically-driven, photothermal, swelling/shrinking, and biologically-driven effects used in 4D printing approaches.

Effects	Details	Stimuli	Examples
Shape memory effect (SME)	An object can memorize its original shape, leading to one-way, two-way, or multiple-way shape changes	Temperature, Light, Magnetic field, Electricity, Humidity, pH	[31–37]
Magnetothermal effect	An object can react to both changes in temperature and magnetic fields.	Magnetic field, Temperature	[38–40]
Magnetically-driven effect	An object can be driven by a magnetic field.	Magnetic field	[41–43]
Photothermal effect	An object can respond to both light and temperature.	Light, Temperature	[44–47]
Swelling/shrinking effect	A volume change of an object can be induced with a water uptake behavior.	Ion concentration, pH value	[48–52]
Biologically-driven effect	An object is driven by biological molecules.	Biological molecules	[53,54]

trachea model. Another group represented 4D-printed vascular stents based on shape memory poly(glycerol dodecanoate) acrylate (PGDA) with T_{trans} in a range of 20°C–37°C, which was suitable for operations in the human body [60]. The PGDA-based stent showed a high fixity ratio at room temperature, a recovery rate of 98% at 37°C, a stable cyclability of more than 100 times, and a rapid recovery speed of 0.4 s at 37°C. In addition, dynamic constructs with shape memory abilities have been manufactured with other types of 3D printers, for example, a shape memory balloon structure based on isobornyl acrylate (IBOA) and aliphatic urethane diacrylate (AUD) by a stereolithography (SLA) printer [35] or a buckminsterfullerene-like structure based on tert-Butyl acrylate (tBA) and di(ethylene glycol) diacrylate (DEGDA) by a digital light processing (DLP) printer [36].

Hydrogel is a network of cross-linked hydrophilic polymer chains and is widely used in biomedical applications with a mimic ability of extracellular microenvironment [61]. It is able to have SME by switching polymeric molecular networks [58]. For example, Chen, Huang and Hu [37] presented shape memory double network hydrogel incorporating polyacrylamide (PAAM) and gelatin (Gel). PAAM network was covalently cross-linked, which served as memorizing an original shape and the Gel network was reversibly cross-linked, which fixed a temporary shape. As seen in Fig. 3(c), the shape memory behavior was examined through the shape deformation with stretching, twisting, and compression. The shape recovery was achieved under 40°C of hot water.

Magnetothermal effect and magnetically-driven effect

The magnetothermal effect describes a performance that results in heat induced by magnetic materials. The magnetothermal mechanism

is categorized as the following three mechanisms of heat generation in magnetic materials: (1) Eddy current loss, (2) hysteresis losses, and (3) relaxation loss, including Neel relaxation, Brown relaxation, and predominant mechanism [62]. The magnetothermal effect employs magnetic and thermosensitive materials to perform dynamic constructs. For example, Liu, Wang, Wu, Dong and Sang [38] employed the magnetothermal effect merging with the SME to induce intelligent products, as seen in Fig. 2(d). The structures based on PLA, thermoplastic PU, and Fe_3O_4 particles were manufactured as a re-entrant structure, which was set as the original shape. It was transferred to a temporary shape by a uniaxial quasi-static compression force at room temperature. When the compressed structure was inserted into an alternative magnetic field (an induction coil), the original shape was recovered within 40 s with an efficacy of 95.5%. With the programmable shape, this procedure has been used to produce intelligent stents. For example, PLA/ Fe_3O_4 tracheal stents were fabricated as a curved rectangle of an S-shaped hinge structure [39] and a bioinspired structure with the entire skeleton of a glass sponge and a fragment of the cage structure [40].

Indeed, the magnetothermal effect requires thermosensitive materials to respond to the temperature increase during the fabrication and design of dynamic constructs. In another aspect, only magnetic materials can perform 4D-printed constructs with the magnetically-driven effect through contactless control of motion. For example, the motion of magnetic hydrogels based on alginate (Alg), methylcellulose (MC), and polyacrylic acid (PAA)-stabilized magnetic nanoparticles (MNPs) of Fe_3O_4 were assessed with various patterns [41]. The cubic-shaped hydrogel with the one-type ink of 20% MNPs performed the highest vertical jump of 8.0 ± 1.0 mm when attracted by a neodymium magnet. The symmetrical patterns of wheel-shaped hydrogel could travel around 50

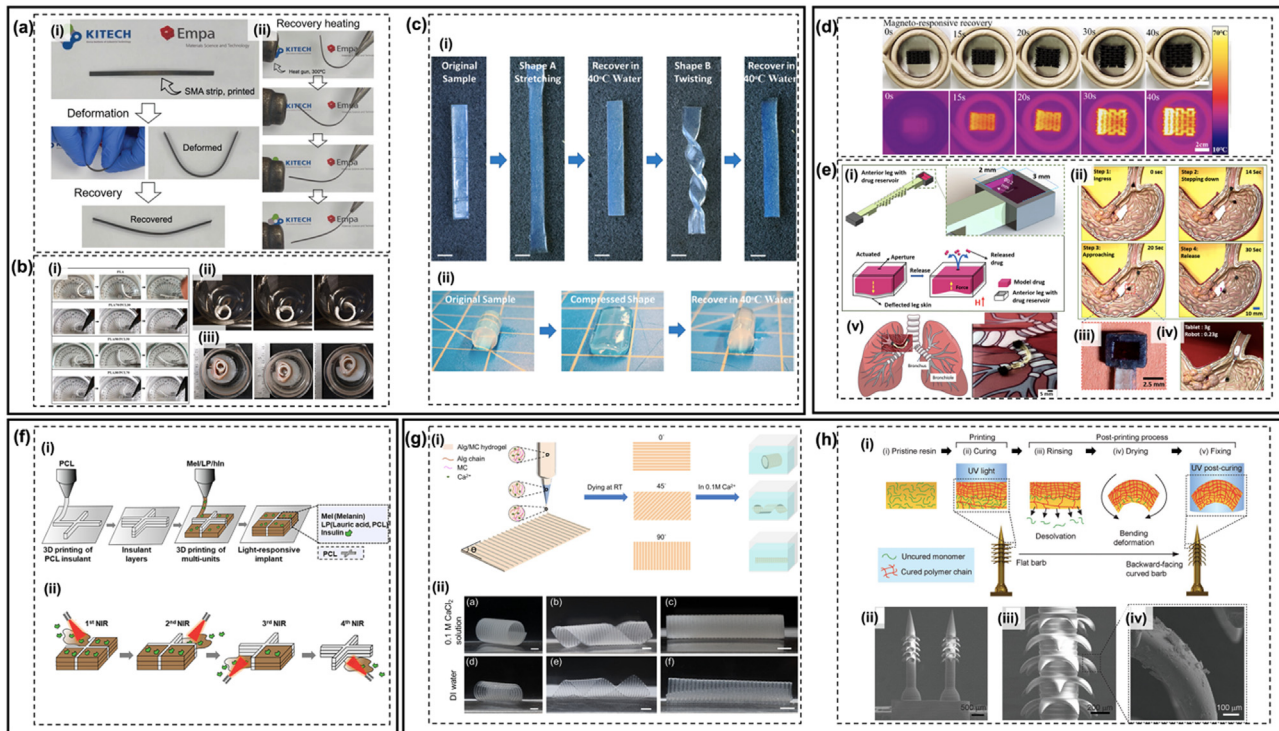


Fig. 2. Shows a conclusive image of effects induced in 4D printing mechanisms, including (a-c) shape memory effects (SME) of alloys, polymers, and hydrogels, (d-e) magnetothermal and magnetically-driven effects, (f) photothermal effect, and (g-h) swelling and shrinking effects, as detailed below. The Fig. is adapted from [32,34,37,38,42,45,48], and [50] with permission of John Wiley and Sons, Elsevier, American Chemical Society and John Wiley and Sons.

- (a) Fe-based strips were able to perform (i) shape deformation and (ii) recovery of SME under heat [32].
- (b) (i) SME of strips based on various ratios of PLA/PCL was induced under the thermally activated stimulus. (ii) The shape transformations of PLA70/PCL30 scaffolds were investigated by placing them inside an incubator and (iii) in a native tracheal [34].
- (c) Shape recovery behaviors of polyacrylamide (PAAM) and gelatin (Gel) hydrogels were investigated using shape deformation techniques, including (i) stretching, twisting, and (ii) compression (scale bar = 0.5 inches) [37].
- (d) A shape memory recovery of a reentrant structure consisting of polylactic acid (PLA), thermoplastic polyurethane (PU), and Fe_3O_4 particles was induced by a magnetic field [38].
- (e) (i) A magnetically-driven soft robot containing a drug reservoir in an anterior leg was used in drug delivery systems (DDSs). The anterior leg was deflected during the influence of the magnetic field, and the drug was released through the small aperture when the magnetic field was turned off. (ii) The assessment of the robot's locomotion was examined inside an anatomical model with target cancer tissue. (iii) The soft robot could contain drugs inside the drug reservoir, and (iv) it could also carry a solid tablet. Moreover, (v) the turning locomotion scenario of the robot was tested on a map of the bronchiole network [42].
- (f) (i) A multiunit implant consisting of melatonin (Mel), lauric acid (LA), polycaprolactone (PCL), and human insulin (hIn) was proposed as a delivery platform. (ii) The hIn was released by triggering with near-infrared (NIR) light [45].
- (g) (i) Patterned hydrogels based on alginate (Alg) and methylcellulose (MC) were fabricated with different configurations, which led to various deformations like (ii) tube, helix, and rolling structures in 0.1 M CaCl_2 and DI water solution (scale bars = 5 mm) [48].
- (h) (i) Bioinspired microneedles were printed by a projection microstereolithography ($P\mu\text{SL}$) process, and a programmable deformation of printed bars was achieved by rinsing, drying, and fixing, which was shown by (ii-iv) SEM images of the microneedle with deformed barbs [50].

cm. This magnetically-driven effect has been widely used to control the direction of a smart robot, which travels to cancer cells for on-demand drug release on the target [42,52,53,63]. For instance, Joyee and Pan [42] presented an untethered soft robot with multi-modal locomotion capability, which was fabricated by a magnetic field-assisted projection stereolithography (M-PSL) technique. The robot was comprised of elastic polymer and iron oxide nanoparticles (IONs). The optimized design of its shape was a body with an anterior leg, a posterior leg, and transverse grooves on the lower and side surfaces. This groove-based design allowed bi-directional locomotion, which manifested the blending angle up to 146°C on a xy plane and the tilt angle to 22°C on a z axis. To produce a drug delivery system, a drug reservoir was inserted into the anterior leg of the robot and covered by a film on the top of the reservoir. The reservoir wall and film were made of the particle-polymer composite, which generated a restrictive capillary force from surface tension to prevent drug leakage. When the robot was moved under the influence of the magnetic field, the bottom of the anterior legs was deflected, and a tension force was applied towards the magnet. The drug would be re-

leased when an up-thrust pressure generated by the turned-off magnetic field overcame the restrictive force, as illustrated in Fig. 2(e-i). The locomotion capability of the robot was proven inside an anatomical stomach model and a lung model, as shown in Fig. 2(e-ii-iv). Furthermore, the advantages of 4D printing in the fabrication of magnetic composites have facilitated the tailored patterns and oriented magnetic domains within the structural design [64]. For example, magneto responsive soft materials with programmed magnetization via mechanically-guided 4D printing were presented [43]. A composite ink based on polydimethylsiloxane (PDMS), crosslinker, catalyst, silica nanoparticles, and NdFeB particles was printed between a series of designed joints on a stretched substrate by a direct ink writing (DIW) technique. The printed structures were magnetized under 3.25T of an impulse field. The shape deformation was activated by removing the magnetized material and joint. The magnetized flat shape was rapidly transformed to a curved shape within 0.2 s under 200 mT of a magnetic field.

The magnetic field has been widely used in biomedical applications because it provides non-invasive management, deep tissue penetration,

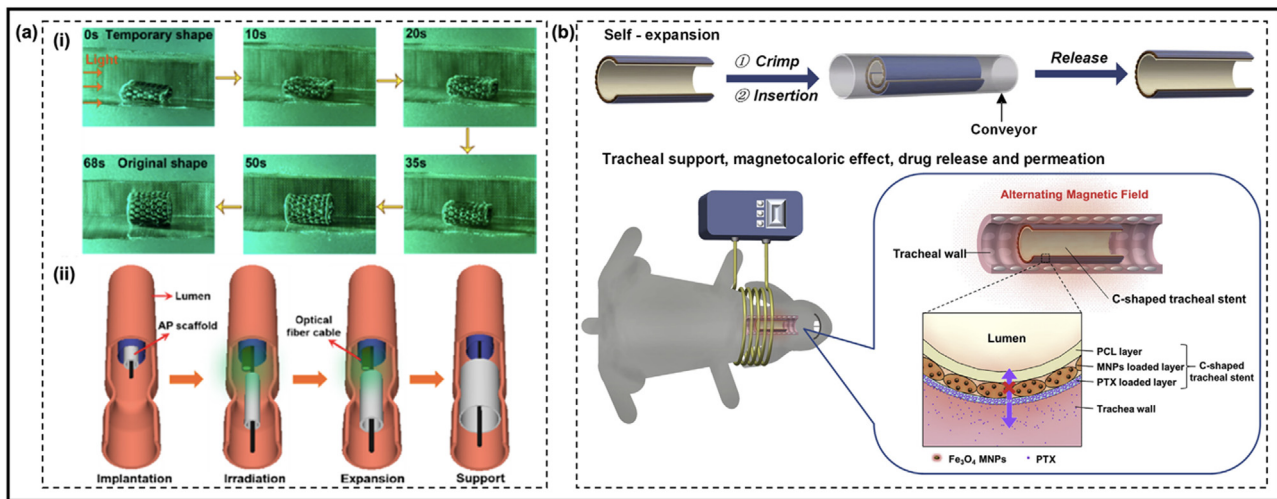


Fig. 3. Shows 4D printing applications in surgical resections. (a) The shape memory scaffolds with an intraluminal structure performed (i) shape recovery under the light stimulus. (ii) The scaffolds were incorporated with an optical fiber cable in the pipeline as a smart device to support the lumen treatment of cancer lesions [70]. (b) A schematic mechanism of a self-expandable C-shape was applied as smart tracheal stents [85]. The Fig. is adapted from [70] and [85] with permission of American Chemical Society and Elsevier.

and a localized heat source [65]. The addition of magnetic materials in constructs can perform remote triggering of shape recovery [33]. Especially the hard-magnetic composites enable the remote control to shape transformation [26,66]. The high amount of MNPs is involved in the faster speed of heat induction and higher temperature [65]. In addition, the magnetic-based constructs have the potential to induce hyperthermia in cancer therapeutics. The incorporation of magnetic composites under high frequencies of an alternating magnetic field (AMF) is able to occur dissipative behavior, which leads to generating heat [26]. The ability of heat generation in the magnetothermal and magnetically-driven effects is a strong advantage for cancer hyperthermia [65]. Likewise, the remote-control abilities are useful for precise positioning control in cancer therapeutics such as drug delivery systems (DDSs) [63,67].

Photothermal effect

The photothermal effect is a phenomenon in which photothermal materials absorb the energy of light and then turn it into heat, causing the raised temperature of materials [68,69]. The heat of the photothermal effect relates to energy loss from an interaction between light and matter molecules. It can be generated from three mechanisms as follows: (i) the plasma resonance effect of metals; (ii) the electron-hole generation and relaxation of semiconductors; and (iii) the molecular orbital excitation and lattice vibration of molecules of carbon- and polymer-based materials [68,69]. The raised heat from the photothermal effect is beneficial for abating cancer cells in photothermal therapy [70]. This photothermal effect is used to induce dynamic constructs by employing light-responsive materials to cause heat and then allow reactions of temperature-responsive materials.

Near-infrared (NIR) light has attended various wavelengths of light in treatments because of noninvasive, spatiotemporal, and deep penetration [71] into the tissue, especially the second region of NIR. [11]. For example, the Gel/Alg/PCL scaffolds coated with PDA showed an excellent photothermal effect in which the temperature was raised to 44°C within 1 min under 0.2 W/cm² illumination. In contrast, the scaffolds without PDA had no temperature increase. The *in vivo* photothermal effect of scaffolds was proven in the subcutaneous area of mice. The temperature of coated PDA scaffolds reached 55°C while the temperature of Gel/Alg/PCL scaffolds was only raised to 42°C [44]. Another strategy of the photothermal effect applied in the control of release was a multiunit implant of protein/antibody/hormone delivery, shown in Fig. 2(f) [45]. The implant was printed as four rectangular

units, which consisted of melanin (Mel), lauric acid (LA), PCL, and human insulin (hIn), with a cross-shaped PCL axis as a center as seen in Fig. 2(f-i). Mel is a NIR-sensitive biopolymer used as a photothermal agent for inducing the photothermal effect. PCL was used to block heat diffusion. The unit irradiated with 1.5 W/cm² of 808-nm NIR laser for 5 min showed a temperature increase from 21.9±1.1°C to 45.4±1.2°C, which resulted in melted LA and loss of the shape of the irradiated unit (Fig. 2(f-ii)). Moreover, bone tissue engineering scaffolds have been developed with 4D printing by providing the perfect shape fitting in the irregular bone defect [46]. The scaffolds consisted of β -tricalcium phosphate (TCP) and thermal-responsive shape memory poly(lactic acid-co-trimethylene carbonate) (P(DLLA-TMC)) with a T_{trans} of 45°C. In addition, black phosphorus nanosheets and osteogenic peptides were loaded into the scaffolds to induce a photothermal effect and osteogenic differentiation. Upon NIR irradiation, the on-demand deformation/recovery of scaffolds was carried out at 45°C and 37°C, respectively. With the abilities of reconfigurable shapes and bone formation support, the scaffolds were useful for narrow paths in bone implantation. Similarly Luo, Lin, Chen and Wei [47] fabricated cell-laden constructs with a shape-morphing ability. The biphasic scaffold consisted of Alg/PDA structures in the middle of the scaffold and cell-laden Alg/gelatin methacryloyl (GelMA) structures at the end. The shape-morphing ability of scaffolds involved the contents of Alg/PDA, by which 70% of alginate/PDA in the scaffold provided a completely folded shape under NIR irradiation with 0.5 W/cm² for 180 s. After shape deformation, the scaffold maintained the deformed shape with high cell viability for at least two weeks.

Swelling and shrinking effects

The swelling/shrinking effect of hydrogel has been driven by water uptake behavior, which is actuated by ion concentrations and pH values [10,72]. It enables the hydrogel to generate shape-morphing ability through the nonuniform internal stress [48]. The swelling/shrinking effect can be programmed by different components across the hydrogel thickness/plane⁴⁸ or different crosslinking densities [49,50]. For example, Alg/MC hydrogels were prepared with different configurations of distributive components in the plane, as seen in Fig. 2(g-i) [48]. The shape-morphing direction was programmed via the printed strip at a specific angle, which affected the elastic tensor. As a result, the shape deformation of hydrogel sheets with the printed strips at various angles of 0°, 45°, and 90° provided a tube-curling structure, a helical structure, and a rolling structure, respectively, as depicted in Fig. 2(g-ii). Simi-

larly, the swelling/shrinking effect has been employed to induce shape deformation of the printed object with different crosslinking densities [49,50]. Cao, Tao, Gong, Wang, Wang, Ju and Zhang [49] demonstrated a 4D-printed hydrogel based on methacrylated alginate (SA-MA) hydrogel. The SA-MA hydrogel showed a step-wise shape deformation when immersed in Ca^{2+} and chitosan solutions because the ion exchange increased crosslinking density, which led to the volume change of hydrogel. In addition, the SA-MA bilayer hydrogels with different degrees of methacrylation could perform various degrees of the shrinking effect in the Ca^{2+} solution. Another group employed the 4D printing technique with the shrinking effect to support complex features of microneedle fabrication [50]. The bioinspired microneedle with backward-facing curved barbs shown in Fig. 2(h) was fabricated by a projection microstereolithography (P μ SL). The photopolymerization of the DLP started on the surface of the precursor solution and gradually propagated into the solution, which generated a gradient of crosslinking density within layers. After the printing process, the uncured monomer in the bottom part of the barbs was diffused out by immersing the microneedle in ethanol, which led to the loosened space in the network. As a result, the bottom part of the barbs shrank, and the barbs bent downward when the microneedle was dried. Finally, the cured shape was fixed by UV exposure.

These effects have been incorporated with other effects, like the SME, to enhance the potential in biomedical applications [51,73]. For instance, a dynamic micro-structure with multi-responsive bilayer membranes consisted of shape memory poly(ϵ -caprolactone)-diacrylates (PCLDA) and hydrogel layers [51]. It was used to control multi-scale structural morphing for bone repair, supporting the potential of bone repair. It could appropriately wrap around the bone defect through the swelling and shape memory effects. Moreover, swelling and shrinkage effects have been induced by a pH stimulus. For example, the swelling behavior of hydrogel-based materials allows shape morphing through deprotonation and protonation [7,52]. To illustrate, hydrogels based on carboxyl groups have occurred the swelling effect at a high pH because the carboxyl group becomes deprotonated and induces electrostatic repulsion forces between molecules. On the other hand, the carboxyl groups perform the shrinkage effect at a low pH because of protonation [52].

Biologically-driven effect

The biological-driven effect refers to behavior caused by biological stimuli like enzymes and cells. The biological stimuli help perform dynamic structures of the 4D printing technique. As previously discussed in the introduction section, the enzyme is another unique factor in the cancer environment. It can thus identify the cancer site in a range of early-stage tumors [24] and facilitate to control drug release in cancer treatments [53,74]. For example, Ceylan, Yasa, Yasa, Tabak, Giltinan and Sitti [53] employed the MMP-2 enzyme in activating drug release. Another group applied enzymes to the enhancement of drug release and the degradation of products inserted in the body [74]. Moreover, sperm cell has gained attention in the applications of drug carriers because sperm is naturally optimized to swim in the reproductive system [75]. For instance, Magdanz, Sanchez and Schmidt [54] created a micro-biorobot that consisted of a microtube and a single cell. The microtube was fabricated by rolling titanium and iron layers [54] with lithography and processing technologies [76]. The magnetic materials incorporated into the microtube enhance the direction control under an external magnetic field. The magnetic field intensity of 22mT at a 2cm distance was well used to guide the microtube. This strategy is sound in drug delivery for gynecological diseases because the sperm could perform drug encapsulation and travel to the target site.

4D printing technologies in cancer therapeutics

The proposed mechanisms of 4D printing approaches are used to drive dynamic structures in potential cancer therapeutic applications,

such as surgical resection, DDSs, hyperthermia, photothermal therapy, and others like a pharmaceutical model. The applications and successes of 4D-printed structures in cancer therapeutics are outlined in Table 2.

Surgical resection

Surgical resection is the direct removal of cancerous tissue. It has been widely used in clinical cancer treatments [71,77]. 3D printing technology in the resection has been used to fabricate devices, models, and scaffolds with the ability to create personalized fabrications. For example, Ock, Kim, Lee, Yang, Kim, Jeong, Choi and Kim [78] printed *in vitro* phantoms to guide skin cancer resection to support a surgical plan. The phantoms could help directly mark information on a patient's skin in an operating room that no other methods had provided before. Furthermore, 3D-printed models have been proven to encourage potential outcomes of surgical therapeutic [79,80] and comprehension of medical information to patients [81]. Besides the models and devices, 3D printing has been used to fabricate implanted scaffolds with multifunctionality for surgical resection. However, resection treatments still risk having residual cancer cells, possibly leading to local recurrence and postsurgical effects [82] such as peritoneal adhesion [83], tissue defects like lumen of cancer lesions [70], and bone defect [84].

4D printing technology can provide dynamic structures to address these concerns about conventional resection and postsurgical effects. Deng, Zhang, Jiang, Liu, Yuan and Leng [70] proposed an intelligent medical device enabling controllable expandable scaffolds under light irradiation. The scaffolds employed the SME of PU to obtain the recovery process and gold nanoparticles (AuNPs) which are a good candidate for photosensitizer in the NIR range [16,18] to achieve the photothermal effect. The PU/AuNPs scaffold was initially compressed to a flat position and rapidly expanded on the targeted lesion site under light stimulation. The intraluminal scaffold was rapidly returned to its original shape within 70 s under light irradiation with 2 W/cm² of intensity, as demonstrated in Fig. 3(a-i). The expandable performance was practical to fulfill tissue defects caused by cancer lesions (Fig. 3(a-ii)). The existing AuNPs also generated heat in the composite scaffolds with the plasma resonance effect under the activation of 520 nm irradiation, which approached photothermal therapy. Additionally, a peritoneal adhesion might occur after peritoneal surgery. 3D-printed disc-like nanogels were used to prevent postsurgical peritoneal tissue adhesions after ovarian cancer surgery [83]. The nanogel based on poloxamer 407 was able to contain paclitaxel and rapamycin. It employed a sol-gel transition of poloxamer 407, which formed sol at 5°C and turned into gel at 37°C to encapsulate and release drugs. The disc-like nanogels were designed to fit in the peritoneal cavity of mice after ovarian surgery and served as a physical barrier by concealing the interface between the surgical incision and the organ. At the same time, drugs were further used to treat residual tumor cells after the surgery. In addition, Chen, Jin, Yang, Liu, Liu, Cai, Shen and Guo [85] designed a 4D-printed C-shape stent, which acted as tracheal support with self-expandable behavior and enabled controlled drug release, as shown in Fig. 3(b). The stent was comprised of inner, middle, and outer layers that are PCL, Fe₃O₄ loaded in PCL, and paclitaxel (PTX) drug loaded in 1-hexadecanol/ethylene-vinyl acetate (EVA) layer. The stent provided good self-expandable behaviors through compression/expansion. It generated heat when 38.7Gs of AMF was applied. As a result, the PTX was released at 43°C, its release was faster than 37°C because of temperature-responsive 1-hexadecanol. The stent was proven by being implanted into a tracheal rabbit. It maintained airway patency for 30 days without mucus or sputum blockages.

Drug delivery systems (DDSs)

Chemotherapy is a drug treatment that uses chemicals or drugs to kill abnormal cells [86]. The biggest concern of conventional chemotherapy is the lack of specific chemotherapeutic drugs for cancer cells because the drug can affect both normal and cancer tissues [17,87]. Be-

Table 2
Advanced applications of the 4D printing technology in the field of cancer therapeutics.

Platforms	Materials	Other carried materials	Additive manufacturing (AM) types	Aims	4D mechanisms	Tissue/Organ	Ref.
Surgical Resection							
scaffold	Gold nanoparticles (AuNPs), Polyurethane (PU)		A high-temperature printed mode of 3D-Bioplotter (direct writing)	The ability of programmable shape was used to support the lesion lumen which could be caused from the postsurgical operation.	- photothermal effect - shape memory effect	cancer lesions	[70]
scaffold	Poly-(ethylene oxide)-b-poly(propylene oxide)-b-poly(ethylene oxide) (PEO-PPO-PEO or poloxamer/pluronic),	Paclitaxel (PTX) and Rapamycin	A fused deposition technology printer	The disc-like nanogels with a reversible sol-gel transition were used to prevent the postsurgical peritoneal adhesion.	- reversible sol-gel transition	ovarian cancer	[83]
stent	Poly(ϵ -caprolactone) (PCL), Fe ₃ O ₄ , 1-hexadecanol/ethylene-vinyl acetate (EVA) copolymer	PTX	An extruder-based 3D printer with a roller bed	The self-expandable performance of C-shape consisted of a PCL layer, a Fe ₃ O ₄ -based layer, and a PTX-loaded layer was induced by an alternative magnetic field (AMF) in order to enhance tracheal treatments. Concurrently, the stimulation with AMF induced the cancer cell death due to heat.	- shape memory effect - magnetothermal effect	malignant tracheal stenosis	[85]
Drug delivery systems (DSSs)							
scaffold	Alginate (Alg), Polydopamine (PDA), Gelatin (Gel)	Doxorubicin hydrochloride (DOX-HCl)	A co-axial 3D printer	A Gel-based core part of core/shell fiber scaffolds served as the control of drug-loaded release under near-infrared (NIR) irradiation.	- photothermal effect - reversible sol-gel transition	breast cancer cells	[71]
scaffold	Alg, Gel, PCL, PDA	DOX-HCl, dexamethasone (DEX)	An extruder-based 3D printer	A Gel-based core part of multilayer core/shell scaffolds served as the control of drug release under NIR irradiation. The PCL and PDA layers protected drug leakage for the long-term incubation.	- photothermal effect - reversible sol-gel transition	breast cancer cells	[44]
microrobot	methacrylamide chitosan (ChMA), iron oxide nanoparticles (IONs)	Azide-modified doxorubicin (DOX)	A two-photon direct laser writing (TDLW) technique	The microswimmer was design to be able to guide locomotion via a magnetic field and control on-demand releasing and dosing with switching the ultraviolet (UV) light on and off	- light- and magnetically-driven effects	breast cancer cells	[74]
scaffold	Alg, ION (Fe ₃ O ₄)	DOX-HCl, Bovine serum albumin (BSA), Human mesenchymal stem cells	A extrude-based 3D printer with a coaxial nozzle	The hollow scaffolds encapsulated drug/protein/live cell in a part of Alg-based core. The on-demand release of these carried materials was induced through shape deformations of the end of ION-based shell under an external magnetic field.	- magnetically-driven effect		[67]
millirobot	poly(N-Isopropylacrylamide) (PNIPAM), laponite nanoclay ([Mg _{5.34} Li _{0.66} Si ₈ O ₂₀ (OH) ₄]Na _{0.66}), and NdFeB magnetic particles	levofloxacin (L830182)	A extrude-based 3D printer	The millirobot was programmed to control locomotion with an external magnetic field. The drug-loaded release was activated by the mechanical centrifugal force which was generated by a rotating magnetic field	- magnetically-driven effect	breast cancer cells	[63]
scaffold	Gel, chitosan, poly(lactic-co-glycolic acid) (PLGA)	5-fluorouracil (5-FU), DOX-HCl	An extrude-based 3D printer	The sponge-like scaffolds employ the specific response in acidic environment to control drug release	- swelling effect (pH-response behavior)	breast cancer cells	[96]

(continued on next page)

Table 2 (continued)

Platforms	Materials	Other carried materials	Additive manufacturing (AM) types	Aims	4D mechanisms	Tissue/Organ	Ref.
microrobot	PNIPAM, poly(acrylic acid) (PAA), polyvinylpyrrolidone (PVP), silicon (Si), and Fe ₃ O ₄	DOX	A femto-second direct laser writing (Fs-DLW) printer	The bioinspired microswimmer was programmed to respond to only acidic environment for controlling drug release. Its locomotion was guided by a magnetic field to reach the targeted site	- magnetically-driven effect - swelling effect (pH-response behavior)	HeLa cells	[52]
microrobot	Gelatin methacryloyl (GelMA), lithium phenyl-(2,4,6-trimethylbenzoyl) phosphinate, ION	Dextran-FITC drug, anti-ErbB 2 antibody	A two-photon direct laser writing system	A direction of the helical microswimmer was controlled under a magnetic field. When reached the targeted site, it could respond to MMP-2 enzyme to release drug.	- magnetically-driven effect - biologically-driven effect	breast cancer cells	[53]
microrobot	dip-in laser lithography photoresist, negative-tone photoresist, Fe, Ti, Bovine sperm cell,	DOX-HCl	A 3D laser lithography	The sperm-hybrid microrobot consisted of microstructure and a sperm cell. The sperm inserted inside the microstructure consisted of a microtube and flexible arms, which act as the drug-loaded sperm release upon hitting with targeted cells.	- magnetically-driven effect - biologically-driven effect	gynecologic cancer treatment	[75]
Hyperthermia scaffold	PNIPAM, nanoclay, ION (Fe ₃ O ₄)		A direct ink writing (DIW) technique	The multiarm hydrogel scaffold generated heat under an AMF due to magnetic composite. It could induce both shape transformation and cell death under AMF.	- magnetothermal effect	human malignant melanoma cells	[65]
Photothermal therapy microrobot	IP-S photoresist, propylene glycol methyl ether acetate (PGMEA), PDA, magnetic nanoparticles (MNPs)		A 3D printing two-photon lithography system	The helical microrobot was programmed to able to guide locomotion with a magnetic field and induce heat under NIR irradiation upon reaching the targeted cancer cells	- magnetically-driven effect - photothermal effect		[102]
device	poly(D,L-lactide-co-ε-caprolactone) methacrylate (poly(DLLA-co-CL)MA), gold nanorods functionalized with poly(ethylene glycol) methyl ether thiol (mPEG-SH) (PEGylated AuNRs)		A digital light processing (DLP) 3D printer	The multifunctional device induced both shape recovery of unfolded shape and heat under NIR irradiation, which were useful to insert devices like a stent into body and kill cancer cells, respectively.	- photothermal effect - shape memory effect	Human lung epithelial cells	[103]
device	titanium (Ti) and polylactic acid (PLA)	Cyanine7 (Cy7), Nile red	a fused filament fabrication (FFF) printer	The device served as anticancer drug carrier and induced radiopacity and photothermal conversion.	- photothermal effect	cancer cells (CT26 cells)	[82]
Others device	poly(ethylene glycol) diacrylate (PEGDA), bisphenol A ethoxylate dimethacrylate (BPADMA)		A projection micro-stereolithography (PμSL).	The shape morphing of cell culture array was used to facilitate the biological insert in the cassette configuration for the glioblastoma patient-derived organoid models	- shape memory effect		[108]
soft robot	non-aqueous photocurable resin Spot E elastic polymer, magnetic nanoparticle (MNPs)	drug solution	A magnetic field assisted projection stereolithography (M-PSL)	The locomotion of soft robot was controlled by a magnetic field in order to travel to the target site. The on-demand drug release was induced with mechanical and magnetic properties by turn on/off the field.	- magnetically-driven effect	targeted cancer site	[42]

sides, the drug concentration is limited by saturation solubility, resulting in insufficient doses [88]. The DDSs have addressed the concerns, which they are one of the localized therapies that minimize drug distribution, leading to fewer side effects on normal tissues. 3D printing has been used to fabricate drug-loading scaffolds for DDS. In addition, 3D-printed scaffolds have been examined with studies of release evaluation in order to DDS applications. For example, patches composed of poly(lactide-co-glycolide) (PLGA), PCL, and 5-fluorouracil (FLU) were fabricated using an extruder-based printer [88]. The patches were proposed as a drug manner with controllable release in a long-term incubation over four weeks. Their drug release was studied through changes in geometric modification. The patches with different pore types provided various FLU releases, and the increased thickness of patches also reduced FLU release. Similarly, the release of FLU drug coated on oral tablets was studied through formulation composite and processing parameters [89]. Another team fabricated microporous scaffolds consisting of intra-strut microscale porosity using porogen leaching and 3D printing [90]. The microscale pore helped slow down the drug release. Besides, a methotrexate (MTX) (4-Amino-10-methylfolate) was incorporated into PLA filaments to enhance the drug's long-term incubation [91]. The PLA/MTX scaffolds maintained the drug for 30 days, and the drug was consistently released over 30 days. Furthermore, 3D printing has been widely used to create pharmaceutical models to understand patients' responses to anticancer drugs and cancer environments by combining live cells into the printing process, which is well-known as 3D bioprinting [92–94]. Indeed, the strong points of 3D-printed scaffolds in DDS have shown the personalized medicine, which can adjust dose and release rate [89,95]; however, the static constructs of 3D printing have limited the on-demand release, controllable dose, or mobile manners.

To enhance chemotherapeutical efficiency, 4D printing has a significant role in achieving the programmable functions of DDSs. The current 4D printing applications in DDS for chemotherapy will be presented through various categories of stimuli, including light, magnetic, pH, and biological stimuli used to activate drug release, as entirely illustrated in Fig. 4.

Light-induced DDSs

The porous scaffolds, like core/shell^{44,71} and hollow [67] have attracted attention in DDSs. The photothermal effect has been utilized to induce 4D-printed constructs through the sol-gel transition. The sol-gel transition enables the constructs to control on-demand drug release. For example, Wei, Liu, Wang and Luo [71] fabricated drug-loading scaffolds comprising core-shell hydrogels, as seen in Fig. 4(a). The scaffolds used PDA/Alg as the shell and Gel as the core parts. Doxorubicin (DOX) drug was loaded into the core part. The PDA induced the photothermal effect under NIR irradiation, which caused a temperature rise in the core-shell scaffolds. The raised heat then activated the sol-gel transition of Gel, which resulted in the release of the drug loaded in the core of Gel hydrogel. The hydrogel with 70%w/v of Gel concentration maintained gel status at 37°C and transformed to sol at 50°C. With the reversible sol-gel transition, the scaffolds could perform on-demand release by turning on/off the laser. As demonstrated in Fig. 4(a-ii), the scaffolds provided the stable photothermal effect under on/off NIR laser illumination with 0.6 W/cm² and 808 nm, which led to efficient control of DOX release. The PDA/Alg scaffolds with loaded DOX proved that *in vitro* 4T1 cancer cells decreased by 80% and *in vivo* tumor volume was significantly reduced. Liu, Wang, Wei, Chen and Luo [44] developed a triple layer of core-shell scaffolds to improve long-term drug delivery. The scaffolds were prepared by printing Gel/Alg mixture and then coated with PCL and PDA (Fig. 4(b-i)). Drugs were added to the matrix, including doxorubicin hydrochloride (DOX-HCl) or dexamethasone (DEX). Gel, PCL, and PDA layers acted as drug encapsulation, drug diffusion barriers, and heat induction to obtain a reversible sol-gel transition for on-demand drug release. The Gel/PCL/PDA scaffolds provided on-demand drug release and controllable dose through light stimuli. As

seen in Fig. 4(b-ii), DOX drug was released according to NIR laser on/off with 808 nm wavelength and 0.3 W/cm², and the drug dose was further controlled with the end of fiber scaffolds. Another group presented a light-triggered DDS of a double-helical microswimmer with a 6 μm diameter and 20 μm length. The microswimmer could control locomotion with the magnetically-driven effect and trigger degradation with the biological-driven effect [74]. It was fabricated using methacrylamide chitosan (ChMA) and superparamagnetic iron oxide nanoparticles (SPIONs) by a two-photon-based 3D printer by which azide-modified DOX drug was bound to amino groups on its surface as shown in Fig. 4(c-i). The ChMA-based microswimmer provided on-demand drug release with a controllable dose under the on/off condition of light stimulation. Approximately 15% of the total drug was released when light (365 nm wavelength and 3.4 × 10⁻¹ W/cm²) was turned on. In comparison, no or slight drug was released when the light was off. The microswimmers were steered with an average speed of 3.34±0.71 μm/s under 4.5 Hz of a 10 mT rotating magnetic field and were partially degradable after 204 hours with no toxic products.

Magnetic-induced DDSs

Wang, Liu, Chen and Luo [67] developed on-demand drug release of scaffolds with the magnetically-driven effect. The scaffolds were designed as hollow fibers consisting of Alg and IONs by a coaxial 3D printer, which enable the encapsulation of drugs, proteins, and living cells into Alg gels in the core part, as shown in Fig. 4(d-i). The on-demand release was induced through deformation under a magnetic field, as illustrated in Fig. 4(d-ii-iv). The higher amount of ION in scaffolds influenced the more excellent deformation process under a magnetic field on/off. DOX drugs were released from the only open ends of fiber under 0.42T of the magnetic field, and no drug was released with the magnetic field off, as seen in Fig. 4(d-v). It implied that fiber could control dose through both open ends of scaffolds and the decrease of Alg concentrations. Another advantage of magneto-responsive materials is the locomotion control with precise positioning under the external magnetic field. The magnetic composites have been widely used to fabricate soft robots in DDSs [52,63] for localized treatments to enhance drug release efficacy and reduce drug resistance. For example, arbitrary hydrogels containing PNIPAM, Laponite nanoclay, and NdFeB magnetic particles could provide temperature and magnetic responses [63]. The hydrogels were designed as leptasteria-like robots and given magnetic moments in the printing process and thermal expansion, which showed various locomotion forms under the magnetic field of a permanent external magnet. The abilities of locomotion were proven through traveling in a stomach model, as demonstrated in Fig. 4(e). The levofloxacin drug was loaded into a robot with leakage prevention under heated water. The mechanical centrifugal force generated by a rotating magnetic field with 800 rpm frequency could enhance drug release.

pH-induced DDSs

The DDSs, as mentioned earlier, are induced with exogenous stimuli; afterward, DDSs induced with a biologically-driven effect will be illustrated. Generally, the pH value of cancer and tumor environment is always particular from normal cells, as mentioned before. The pH value is another factor that can induce some changes in materials, like the swelling/shrinkage effect [52]. Shi, Cheng, Wang, Chen, Wang, Li, Tan and Tan [96] fabricated intelligent scaffolds based on PLGA, Gel, and chitosan. Gel and chitosan were crosslinked by a glutaraldehyde solution to form a pH-responsive imine bond, which respond in an acidic environment. As a result, DOX and FLU drugs were rapidly released at pH 6.5 and 5, whereas slight drugs were released at pH 7. Also, the scaffolds loaded with drugs explicitly showed the efficiency of reducing tumor volume. The pH-responsive scaffolds have been improved with controllable locomotion abilities like soft robots. Microrobots have great attention for manipulating smaller particles, such as single cells, bacteria, and hard-to-reach areas in the body, which leads to precisely targeted delivery [52,53]. The animal-inspired designs and fabrications of 4D-printed

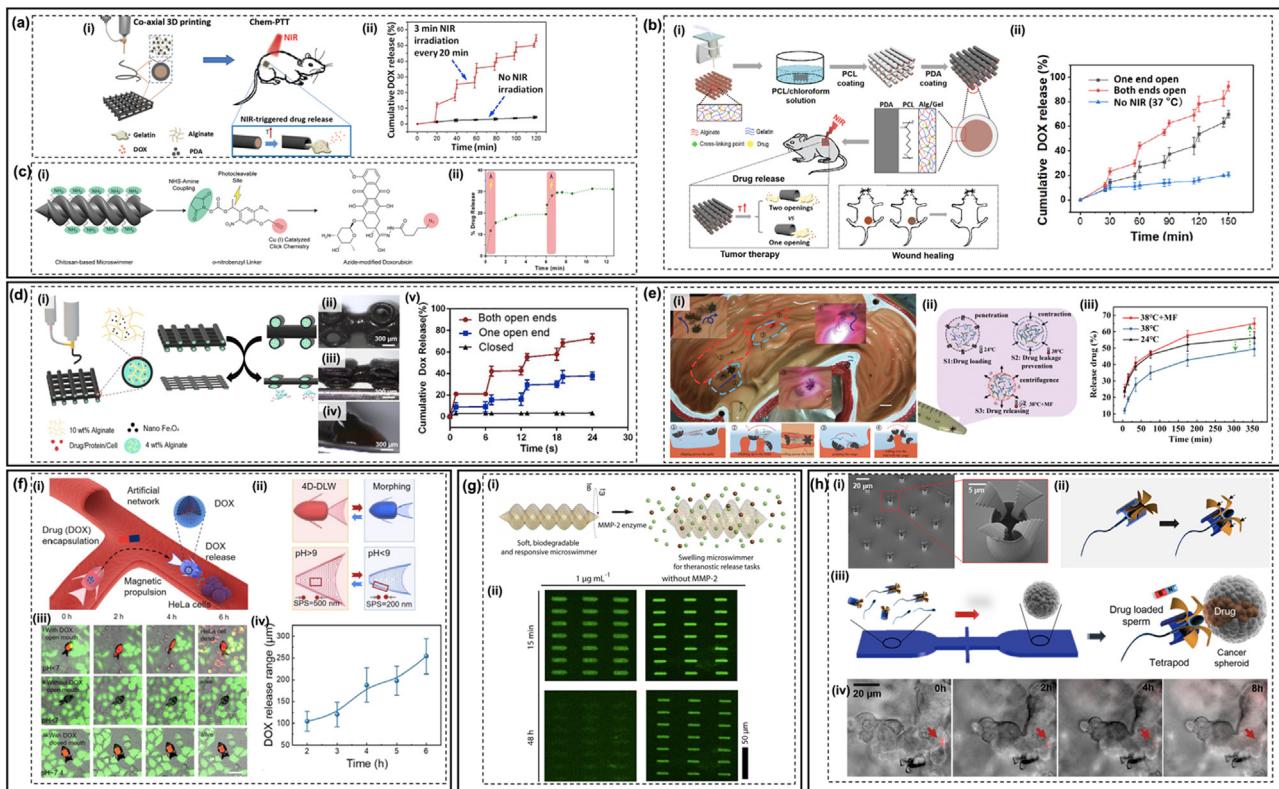


Fig. 4. Demonstrates potential applications of 4D printing in drug delivery systems (DDSs) in which drug releases were triggered by various stimuli, including (a-c) light-triggered, (d-e) magnetic-triggered, (f) pH-triggered, (g) enzyme-triggered, and (h) biologically-triggered drug release of DDSs, as detailed below. The Fig. is adapted from [71,44,74,67,63,52,53], and [75] with permission of Elsevier and American Chemical Society, respectively.

(a) (i) The core/shell scaffold was fabricated by a co-axial 3D printing, which induced the reversible sol-gel transition by NIR irradiation and (ii) examined NIR-triggered release of doxorubicin (DOX) drug from the scaffolds with and without the NIR irradiation with 0.6 W/cm^2 .

(b) (i) The multilayer scaffold based on gelatin (Gel), polycaprolactone (PCL), and polydopamine (PDA) was fabricated by an extruder-based 3D printing with a coating method. (ii) The cumulative DOX drug release was examined with and without the influence of NIR irradiation on the ends of scaffolds [44].

(c) (i) The light-triggered microswimmer embedded DOX via the reaction between amino groups and the NHS group of the *o*-nitrobenzyl linker, which (ii) around 15% of the DOX was released per minute from the microswimmer under 365 nm wavelength of light exposure [74].

(d) (i) The magnetically-driven hollow scaffold was fabricated by using a coaxial-nozzle extruder printer with 10wt% of alginate and iron oxide nanoparticles (IONs) as the shell part and drug/protein/cells loaded with 4wt% alginate as the core part. (ii-iv) The mechanism of drug release was induced by magnetic stimulation, which led to (v) cumulative DOX drug released from the scaffolds with both open ends, one open or closed ends for each hollow fiber of scaffolds [67].

(e) Multifunctional millirobots with a leptasteria-like shape had proven (i) controllable locomotion in stomach model (scale bar is 6mm) and (ii) drug loading/release under different conditions: soaking hydrogel in the levofloxacin solution at 24°C, heating hydrogel at 38°C and the addition of magnetic field (MF) which led to (iii) various drug releases [63].

(f) (i) A concept of the shape-morphing microswimmer with the pH-triggered drug release was applied in DDSs of cancer treatments. (ii) The shape-morphing microfish was fabricated with various point densities inside the body's microfish, which involved with shape-morphing. (iii) The shape-morphing microfish delivered drugs to HeLa cells under different environmental pH levels and various conditions (with DOX drug and mouth opened, without DOX and mouth opened and with DOX and mouth closed). (iv) the quantitative amount of DOX drug was released over 6 hours. (the scale bar = $50 \mu\text{m}$) [52].

(g) (i) The helical microswimmer which could control its motion under a magnetic field, its drug release, and its degradation with MMP-2 enzyme was applied in DDSs. (ii) Epifluorescence images showed dextran-FITC drug release of the microswimmers under different conditions. At $1 \mu\text{g/mL}$ of MMP-2, the microswimmers' size increased and almost all drug was released within 48 hours while the conditions without MMP-2 obviously showed the residual microswimmer [53].

(h) the sperm-hybrid micromotors were used in DDSs to treat cancer cells. (i) Scanning electron microscope (SEM) images of microstructures consisting of a tubular body and four flexible arched arms. (ii) The mechanism illustration of drug-loaded sperm release when exposed to the targeted cell. (iii) The schematic assessment of the delivery and release efficiencies of the drug-loaded sperms on a microfluidic chip, in which the sperm-hybrid drug delivery system was added on one side of the chip and a HeLa spheroid would be inserted on another one. (iv) Images of DOX-HCl distribution in the HeLa spheroid (the red arrows pointed at the sperm head.) [75].

microrobots were used to fabricate smart microrobots in DDSs [52]. The microrobots were inspired by the opening-closing of fish mouths and claw crabs. They controlled drug release through shape-morphing behavior under pH stimuli and propelled with magnetic propulsion, as shown in Fig. 4(f-i). The shape-morphing was conducted with programmable expansion rates determined by the porosity of printed parts (Fig. 4(f-ii)). To prove drug release with shape-morphing behavior, microfish was fabricated by a femto-second direct laser writing (Fs-DLW) and based on PNIPAAm, PAA, polyvinylpyrrolidone (PVP), and Fe_3O_4 . DOX drugs were loaded and encapsulated by immersing in en-

vironmental pH changes. The drug was released through opened and closed mouths of microfish in a slightly acidic solution and pH~7.4 like phosphate-buffered saline (PBS), respectively. The microfish was controllably steered into HeLa cell clusters with permanent ferromagnets, and the drug was only released in an acidic environment in a cell $250 \mu\text{m}$ away from microfish over 6 h, as depicted in Fig. 4(f-iii-iv).

Enzyme-induced DDSs

The enzyme is a pathological marker in a cancer environment and another stimulus used to control drug release. Ceylan, Yasa, Yasa, Tabak,

Giltinan and Sitti [53] utilized the MMP-2 enzyme to induce drug release and IONS to allow mobile abilities for localized cancer treatments as shown in Fig. 4(g-i). MMPs enzyme has been reported as a potential biomarker for breast cancer [25]. The double helical microswimmer based on GelMA and SPIONs was fabricated by a direct laser writing system with a two-photon polymerization and loaded with a dextran-FITC drug [53]. The microswimmer locomotion could control under 20 mT of a rotating magnetic field. The average speed was $3.36 \pm 0.71 \mu\text{m/s}$, and the velocity linearly increased with increasing frequency, which was adjusted following various behavior like cork-screw or step-out movements. $0.125 \mu\text{m/mL}$ was at least the MMP-2 concentration that the microswimmer began to induce the swelling within 20 min. While the swelling behavior instantly began at $1 \mu\text{g/mL}$ of MMP-2, which rapidly increased the microswimmer volume, as seen in Fig. 4(g-ii). The volumetric expansion boosted drug release, ultimately released after complete degradation. In addition, anti-ErbB 2 antibody was able to carry into the microswimmer to delivery at targeted sites.

Cell-induced DDS

Xu, Medina-Sánchez, Magdanz, Schwarz, Hebenstreit and Schmidt [75] developed drug delivery vehicles that were driven and guided by sperm cells and magnetic-based composite. These sperm hybrid micro-robots consisted of the bovine sperm cell and a printed magnetic microstructure. The sperm served as a propulsion source and drug carrier, while the microstructure controlled the sperm liberation. It consisted of a tubular body and four flexible arched arms (Fig. 4(h-i)), which was fabricated using 3D laser lithography and coated with Fe and Ti. The arms would bend when hit with an outer boundary of cells and then open a way to liberate the sperm cells (Fig. 4(h-ii)). The loading ratio of encapsulated DOX-HCl into sperms with the original amount of DOX-HCl in solution was around 15%. The average DOX-HCl encapsulation was 15 pg per single cell. The sperm provided stable *in vitro* encapsulation with less than 10% drug leakage into the medium after 8 h. *In vitro* drug delivery efficiency on HeLa spheroid was tested in a microfluidic chip, as seen in Fig. 4(h-iii). The locomotion of sperm-driven micro-robots was induced under an external magnetic field of roughly 5 mT. After 8 h, the size of the HeLa spheroid was contracted and decreased by around 40% (Fig. 4(h-iv)), indicating the early stage of cell apoptosis. The drug released into the spheroids achieved 87% cell-killing efficiency within 72 h.

Hyperthermia and photothermal therapy

Generally, cell death has been induced under 42°C - 46°C of tissue temperature for 10 min [16]. Hyperthermia is a form of thermal ablation in cancer treatments, which employs a higher temperature (than body temperature) to kill cancer cells [17]. Hyperthermia is induced by various stimuli, such as light, magnetic field, ultrasound, and electrical current. It has great attention with minimal invasiveness, high specificity, and repeatability [82,97]. The light-induced hyperthermia can be called photothermal therapy. It is another type of thermal ablation with a higher temperature, which is induced with various wavelengths of light. On the other hand, photothermal therapy is called a specific form of hyperthermia [97]. Both are extremely useful in treating hard-to-reach areas [18]. Significantly, the light in the NIR-I range (750-900 nm) has attracted attention because of good biological penetration, and another in the NIR-II range (1000-1700 nm) allows deeper tissue penetration [16].

3D printing has played an essential role in two functions: (i) producing personalized structures that support hyperthermia procedures, and (ii) fabricating implanted scaffolds that enable induction to generate heat for hyperthermia. In applications of personalized structures, 3D printing has facilitated individual devices and models, such as immobilization devices [98], flexible antenna [99], and patient-specific replica [100]. In aspects of scaffold fabrication, 3D printing has been used

to fabricate multifunctional scaffolds of light-sensitive and magnetic-sensitive composites, which caused the temperature to increase. The scaffolds provided heat used to kill cancer cells and support tissue regeneration. For example, He, Dong, Yu, Chen and Hao [101] fabricated CaPCu scaffolds incorporating CaCO_3/PCL scaffolds that were decorated with Egyptian blue ($\text{CaCuSi}_4\text{O}_{10}$). The Egyptian blue was added to achieve heat on scaffolds with the second NIR stimulation. The raised heat could damage osteosarcoma (OS) that is a primary malignant bone tumor, and the scaffolds also enhanced osteogenesis.

These 3D-printed structures can be further improved by merging the existing benefits of 3D printing with the controllable response of smart materials to stimuli. 4D printing has transcended the limitations of static printed structures and offered advanced fabrications of scaffolds with on-demand functions, like mobile robots [102], scaffolds with shape transformation [65], and smart devices with shape memory behavior [70,103] upon specific stimuli. Recent 4D printing applications in hyperthermia and photothermal therapies shown in Fig. 5 have been presented.

Hyperthermia

Magnetic materials can induce shape transformation in thermosensitive materials and cell death with hyperthermia. For instance, 3D-printed structures were developed by incorporating magnetic hydrogel and an elastomer layer to achieve programmable shape transformation, as seen in Fig. 5(a) [65]. The structures were designed as multi-arm structures with a double layer of magnetic hydrogel and elastomer, composed of PNIPAM/Fe₃O₄ and silicone/nanosilica/benzophenone, respectively, and interfacially linked with covalent bonds on the interface. Then, under an AMF actuation, the arm was induced to undergo shape deformation by bending up and then holding the hydrogel matrix of GelMA that encapsulated human malignant melanoma (A375) cancer cells. The stimulation of AMF at 230 A of current provided steady heat above 50°C temperature for 20min on the surface of the magnetic hydrogel. The raised heat induced A375 death by reaching 50% during the deformation.

Photothermal therapy

Light is another stimulus used to induce dynamic constructs and allow heat induction in photothermal therapy for cancer treatments. For example, the fabrication of a multifunctional device that provided both shape memory behavior and heat upon NIR irradiation was discovered [103]. The device based on gold nanorods (AuNRs) and poly(D,L-lactide-co-ε-caprolactone) methacrylate (poly(DLLA-co-CL)MA) was fabricated by a DLP printer. The composite performed a fast and stable NIR response, reaching 55°C within 20 sec after 808-nm laser exposure at a power density of about 4.1 W/cm^2 . It returned to the original shape at room temperature within 1 min after the laser was off. However, the composite provided 40 - 45°C of raised temperature after the laser exposure for 5-15 min when it was tested in water at 37°C . With shape memory function, it was proposed as an intelligent stent. The composited-based stent was able to fix its temporary shape above its T_{trans} and cooled to -20°C . The stent inserted in a porcine intestinal segment was heated up with NIR exposure, which could open the intestine within 40 s (Fig. 5(b)). Similarly, Deng, Zhang, Jiang, Liu, Yuan and Leng [70] presented PU/AuNPs-based smart devices mentioned earlier in the surgical resection, which achieved photothermal therapy while inducing shape recovery under 520 nm light exposure. The scaffold contained AuNPs colloid in PU solution heated up to T_{trans} of the composite, 45°C , within 9 s under 2 W/cm^2 of the light irradiation. The reaching time of T_{trans} was different according to AuNPs concentration and light density. In *in vitro* treatment, the survival of breast cancer cells was below 10% under light irradiation at the PU/AuNPs scaffold for 150s. Furthermore, the printed constructs that induce heat used in photothermal therapy have been improved to perform multimodal therapy. An intelligent platform that enabled on-demand drug delivery along with positional detectability and photothermal therapy was encountered [82]. It

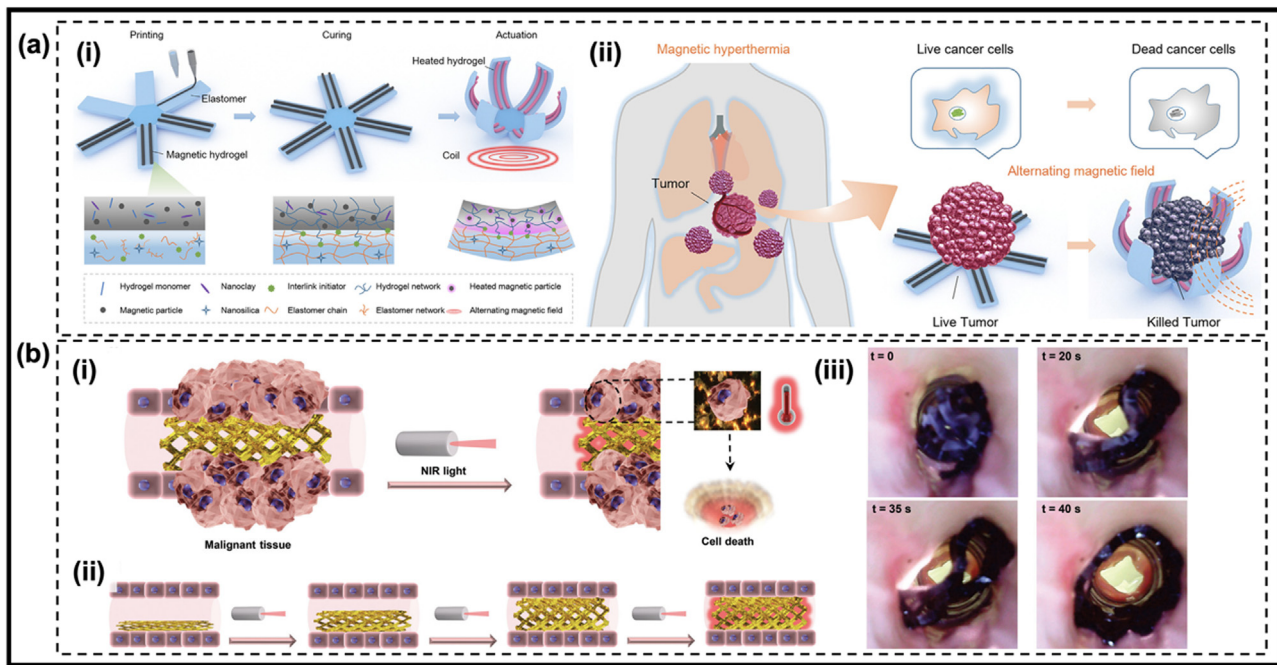


Fig. 5. Shows advanced applications of 4D printing in hyperthermia and photothermal therapies. (a) shows schematic images of fabrication processes and applications of magnetic hydrogels. (i) The hydrogels were fabricated via an extruder-based printer, a curing step, and a shape transformation under an alternating magnetic field (AMF). (ii) The hydrogel with abilities of deformation and heat induction was applied in magnetic hyperthermia. The magnetic hydrogel could induce both shape deformation and cancer cell death under the AMF [65]. (b) The shape memory polymer/Au-based stent that was inserted into a tubular organ could induce (i) photothermal and (ii) shape memory effects (SMEs) with near-infrared (NIR) stimulus for cancer treatments, (iii) which was examined by inserting the composite stent in the porcine intestinal segment [103]. The Fig. is adapted from [65] and [103] with permission of Elsevier and John Wiley and Sons, respectively.

consisted of bullet-shaped composites of Ti and PLA, which had good radiopacity. Upon 808 NIR irradiation, the PLA/Ti bullet temperature was increased by more than 45°C with the increase in Ti proportion. It was limited to 10% vol, which above 10% vol had not significantly shown the difference in the temperature increase. The Nile red was prepared by adding LA and stearic acid (SA) mixture to the printed bullet. The variable temperature under on/off NIR irradiation enabled the platform to control the release behavior of Nile red and Cyanine7 (Cy-7) loaded in the bullet. The bullets noticeably induced apoptosis of murine colorectal carcinoma cells (CT-26 cells) via *in vitro* and *in vivo* evaluation. Another group presented a magnetically-driven helical microrobot with 180 μm of length and 90 μm of outer diameter, which was fabricated by a 3D printer with a two-photo lithography system [102]. It was coated with PDA and MNPs to achieve the photothermal effect and allow magnetic control. Under external electromagnetic actuation, it was controlled along the circular, square, and diamond paths with a speed velocity of 0.278, 0.143, and 0.125 mm/s, respectively. The microrobot provided 71.87°C of raised temperature when exposed to 5 W/cm² of 808 nm NIR irradiation for 120 s, which was sufficient to damage cancer cells.

Other approaches

3D printing is significant in therapeutical devices or models, such as a self-propelled robot for corrector cancer (CRC) [21], a monolithic 3D microfluidic device [104], and anatomical or pharmaceutical models. Among the various fabrications in cancer diseases, there are recent applications of 4D bioprinting in the pharmaceutical model. Regarding the pharmaceutical models, bioprinting has considerable interest with an advanced fabrication of biological structures with multiple cells/drugs to mimic tumor microenvironment closely [105,106]. 4D bioprinting is defined as the fabrication of dynamic biological structures, which directly print biological cells with smart materials in the same procedure. It has attracted considerable attention in biomedical applications [6,107]. In

the field of cancer diseases, it was used to fabricate innovative biological inserts for cell culture and histology [108,109]. Chadwick, Yang, Liu, Gamboa, Jara, Lee and Sabaawy [108] fabricated 4D-printed cell-culture arrays with the self-transformable ability, which was used in a glioblastoma patient-derived model to assess the drug responses. The arrays were made from thermoresponsive shape memory poly(ethylene glycol) diacrylate (PEGDA) and Bisphenol A ethoxylate dimethacrylate (BPADMA) by crosslinking polymeric network with covalent bonds. The PEGDA-based array was able to perform a temporary shape at room temperature and revert to its original shape at 50°C. The arrays with the ability of programmable shape morphing consisted of interconnected wells, allowing insertion processing in only one step. Moreover, this strategy was proposed as intelligent equipment to evaluate the potential of immunotherapy.

Challenges and future perspectives

The 4D printing technique has been utilized in the advanced fabrication of dynamic constructs that respond to specific stimuli, enabling the attainment of on-demand functions like controllable locomotion, programmable shape transformation, on-demand carrier, or degradation. These capabilities are of great significance roles in improving various applications of 4D printing. In cancer therapeutics, 4D printing participates in enhancing localized treatments on targeted sites because of the dynamic constructs' specific responses and controllable abilities. Additionally, it has the potential to evaluate the therapeutic process to the next level. 4D printing has been proposed as a new alternative to enhance the precision of cancer therapies [29,52,53]. The significant potentials of 4D printing applications in cancer therapeutics have manifested in this review through surgical resection, DDSs, hyperthermia, photothermal therapy, and pharmaceutical model. Nevertheless, this technology remains in its initial stage and has encountered challenges.

First, the practical uses of 4D printing in cancer therapeutics remain novel. There are *in vitro* results of 4D-printed constructs in therapeutics;

however, the examinations of *in vivo* situations and human scale have still lacked and been expected in the future to assess clinical use. Second, the insight of smart materials and the response's body on smart materials are questionable. The use of the materials in the biomedical field has specific properties such as biocompatibility, cytotoxicity, and mechanical properties [8]. For example, the magnetic material is useful to induce hyperthermia, guide motion, and trigger shape transformation; however, it should be suspicious with *in vivo* long-term safety and cytotoxicity [65].

In another term of applying stimuli, the normal tissue should not experience side effects as a result of stimulations. Determining the targeted area is crucial in cancer therapeutics because cancer tissue is surrounded by normal tissue. For example, the photothermal effect generates heat on materials, which are used to induce dynamic constructs and cure cancer cells. The heating temperature should not exceed the normal tissues' tolerance level. Excessive heat might affect normal tissue and lead to unexpected results. The temperature used in implantation applications should range from 20°C to 37°C to prevent harm to the body [58]. There are so attempts to decrease T_{trans} as presented before and material size. Like, nanomaterials can reduce the defined region of heat to the nanoscale [68].

Finally, 4D printing is an interdisciplinary technique [4] that requires design skills, manufacturing processes, material understanding, and modeling skills. The biological microenvironment is also complicated and heterogeneous for each patient [8]. The following challenges of 4D printing are design strategies for smart materials to achieve on-demand functions of dynamic structures after the printing process and models of the statistically significant behavior of response situations. The manufacture of 4D-printed structures is limited by real-time knowledge [110]. Artificial intelligence (AI) and its subset, machine learning (ML), have been recommended as powerful tools to improve the abilities of 4D printing [110,111]. In particular, Lin, Chou, Cheng, He, Monteiro-Riviere and Riviere [111] presented the efficiency of nanoparticle delivery on cancers and tumors, which was predicted by multiple ML. Likely, the incorporation of AI and ML into 4D printing has supported the advancement of cancer research in the future.

Conclusion

4D printing has emerged in advanced fabrications of dynamic constructs for various applications. In this article, we have presented an overview of the mechanisms of 4D printing approaches and the prospective of 4D printing in cancer therapeutics. The mentioned applications have already demonstrated the potential of 4D printing techniques in cancer therapeutics. It discussed how emerging 4D printing will play a part in being an innovative alternative in future development of cancer investigations. Furthermore, the current 4D printing techniques in cancer therapeutics, including the insight study of smart materials, the development of biocompatible dynamic structures in the body, the enhancement of design strategies in 4D printing, the material efficiency model for cancer, and the associated challenges and future perspectives, have been presented. It is expected that, as time goes, the 4D printing technology, incorporation with data science and engineering modeling and simulation skills, will be capable of producing even more complex biostructures, which will enhance its application in the field of cancer research and therapies.

Declaration of Competing Interest

No conflict of interest exists.

CRediT authorship contribution statement

Atchara Chinnakorn: Investigation, Writing – original draft, Validation. **Wiwat Nuansing:** Funding acquisition, Project administration. **Mahdi Bodaghi:** Conceptualization, Investigation, Writing – review &

editing. **Bernard Rolfe:** Writing – review & editing. **Ali Zolfagharian:** Conceptualization, Project administration, Investigation, Writing – original draft.

Funding

No funding was received for this work.

Acknowledgments

This work was partially supported by Suranaree University of Technology, Thailand Science Research and Innovation (TSRI), National Science, Research, and Innovation Fund (NSRF) (NRIIS number 179322), and Deakin University. Atchara Chinnakorn was supported by the Science Achievement Scholarship of Thailand (SAST).

References

- [1] Khalid MY, Arif ZU, Ahmed W, Umer R, Zolfagharian A, Bodaghi M. 4D printing: technological developments in robotics applications. *Sens Actuators, A* 2022;343:113670 2022/08/16/. doi:10.1016/j.sna.2022.113670.
- [2] Arif ZU, Khalid MY, Ahmed W, Arshad H. A review on four-dimensional (4D) bioprinting in pursuit of advanced tissue engineering applications. *Bioprinting* 2022;27:e00203 2022/08/01/. doi:10.1016/j.bprint.2022.e00203.
- [3] Khalid MY, Arif ZU, Ahmed W. 4D Printing: technological and manufacturing renaissance. *Macromol Mater Eng* 2022;307(8):2200003. doi:10.1002/mame.202200003.
- [4] Bodaghi M, Zolfagharian A. 1 - 4D printing principles and manufacturing. In: Bodaghi M, Zolfagharian A, editors. *Smart Materials in Additive Manufacturing*. Elsevier; 2022. p. 1–17.
- [5] Melocchi A, Ubaldi M, Cerea M, et al. Shape memory materials and 4D printing in pharmaceuticals. *Adv Drug Deliv Rev* 2021;173:216–37 2021/06/01/. doi:10.1016/j.addr.2021.03.013.
- [6] Arif ZU, Khalid MY, Zolfagharian A, Bodaghi M. 4D bioprinting of smart polymers for biomedical applications: recent progress, challenges, and future perspectives. *React Funct Polym* 2022;179:105374 2022/10/01/. doi:10.1016/j.reactfunctpolym.2022.105374.
- [7] Yang Y, Zeng W, Huang P, Zeng X, Mei L. Smart materials for drug delivery and cancer therapy. *VIEW* 2021;2(2):2020042. doi:10.1002/VIEW.20200042.
- [8] Zhou W, Qiao Z, Nazarzadeh Zare E, et al. 4D-printed dynamic materials in biomedical applications: chemistry, challenges, and their future perspectives in the clinical sector. *J Med Chem* 2020;63(15):8003–24 2020/08/13. doi:10.1021/acs.jmedchem.9b02115.
- [9] Wang Y, Cui H, Esworthy T, Mei D, Wang Y, Zhang LG. Emerging 4D printing strategies for next-generation tissue regeneration and medical devices. *Adv Mater* 2022;34(20):2109198. doi:10.1002/adma.202109198.
- [10] Lui YS, Sow WT, Tan LP, Wu Y, Lai Y, Li H. 4D printing and stimuli-responsive materials in biomedical aspects. *Acta Biomater* Jul 1 2019;92:19–36. doi:10.1016/j.actbio.2019.05.005.
- [11] Chen Y, Zhang J, Liu X, et al. Noninvasive *in vivo* 3D bioprinting. *Sci Adv* 2020;6(23):eaba7406. doi:10.1126/sciadv.aba7406.
- [12] Li R, Ting Y-H, Youssef SH, Song Y, Garg S. Three-dimensional printing for cancer applications: research landscape and technologies. *Pharmaceuticals* 2021;14(8):787.
- [13] Arif ZU, Khalid MY, Noroozi R, Sadeghianmaryan A, Jalalvand M, Hossain M. Recent advances in 3D-printed polylactide and polycaprolactone-based biomaterials for tissue engineering applications. *Int J Biol Macromol* 2022;218:930–68 2022/10/01/. doi:10.1016/j.ijbiomac.2022.07.140.
- [14] Arif ZU, Khalid MY, Sheikh MF, Zolfagharian A, Bodaghi M. Biopolymeric sustainable materials and their emerging applications. *J Environ Chem Eng* 2022;10(4):108159 2022/08/01/. doi:10.1016/j.jece.2022.108159.
- [15] Noroozi R, Zolfagharian A, Fotouhi M, Bodaghi M. 7 - 4D-printed shape memory polymer: modeling and fabrication. In: Bodaghi M, Zolfagharian A, editors. *Smart Materials in Additive Manufacturing*. Elsevier; 2022. p. 195–228.
- [16] Zhang Y, Zhang S, Zhang Z, et al. Recent progress on nir-ii photothermal therapy. *Front Chem* 2021;9 728066-728066. doi:10.3389/fchem.2021.728066.
- [17] Debela DT, Muzazu SG, Heraro KD, et al. New approaches and procedures for cancer treatment: current perspectives. *SAGE Open Med* 2021;9 20503121211034366-20503121211034366. doi:10.1177/20503121211034366.
- [18] Vodyashkin AA, Rizk MGH, Kezimana P, Kirichuk AA, Stanishvskiy YM. Application of gold nanoparticle-based materials in cancer therapy and diagnostics. *ChemEng* 2021;5(4):69.
- [19] Sung H, Ferlay J, Siegel RL, et al. Global cancer statistics 2020: GLOBOCAN estimates of incidence and mortality worldwide for 36 cancers in 185 countries. *CA Cancer J Clin* 2021;71(3):209–49. doi:10.3322/caac.21660.
- [20] Anirudhan TS, Mohan AM. Novel pH switchable gelatin based hydrogel for the controlled delivery of the anti cancer drug 5-fluorouracil. *10.1039/C3RA47991A*. *RSC Adv* 2014;4(24):12109–18. doi:10.1039/C3RA47991A.
- [21] Osawa K, Nakadate R, Arata J, et al. Self-propelled colonoscopy robot using flexible paddles. *IEEE Robot Automat Lett* 2020;5(4):6710–16. doi:10.1109/LRA.2020.3017476.

- [22] Liu H, Yang F, Chen W, et al. Enzyme-responsive materials as carriers for improving photodynamic therapy. *Front Chem* 2021;9:763057. doi:10.3389/fchem.2021.763057.
- [23] Heshmati Aghda N, Dabbaghianamiri M, Tunnell JW, Betancourt T. Design of smart nanomedicines for effective cancer treatment. *Int J Pharm* 2022;621:121791. doi:10.1016/j.ijpharm.2022.121791.
- [24] Liang S-L, Chan DW. Enzymes and related proteins as cancer biomarkers: a proteomic approach. *Clin Chim Acta* 2007;381(1):93–7. doi:10.1016/j.cca.2007.02.017.
- [25] Zununi Vahed S, Salehi R, Davaran S, Sharifi S. Liposome-based drug co-delivery systems in cancer cells. *Mater Sci Eng C Mater Biol Appl* 2017;71:1327–41 Feb 1. doi:10.1016/j.msec.2016.11.073.
- [26] Lucarini S, Hossain M, Garcia-Gonzalez D. Recent advances in hard-magnetic soft composites: synthesis, characterisation, computational modelling, and applications. *Comp Struct* 2022;279:114800. doi:10.1016/j.compstruct.2021.114800.
- [27] Yarali E, Baniasadi M, Zolfagharian A, et al. Magneto-/electro-responsive polymers toward manufacturing, characterization, and biomedical/ soft robotic applications. *Applied Materials Today* 2022;26:101306. doi:10.1016/j.apmt.2021.101306.
- [28] Bastola AK, Hossain M. A review on magneto-mechanical characterizations of magnetorheological elastomers. *Comp Part B* 2020;200:108348. doi:10.1016/j.compositesb.2020.108348.
- [29] Moroni S, Casertari L, Lamprou DA. 3D and 4D Printing in the Fight against Breast Cancer. *Biosensors* 2022;12(8):568.
- [30] Sahafnejad-Mohammadi I, Karamimoghdam M, Zolfagharian A, Akrami M, Bodaghi M. 4D printing technology in medical engineering: a narrative review. *J Brazilian Soc Mech Sci Eng* 2022;44(6):233. doi:10.1007/s40340-022-03514-x.
- [31] Kim T, Lee Y-G. Shape transformable bifurcated stents. *Sci Rep* 2018;8(1):13911. doi:10.1038/s41598-018-32129-3.
- [32] Kim D, Ferretto I, Leinenbach C, Liu W. 3D and 4D printing of complex structures of Fe[Mn]Si-based shape memory alloy using laser powder bed fusion. *Adv Mater Interfaces* 2022;9(13):2200171. doi:10.1002/admi.202200171.
- [33] Jia H, Gu S-Y, Chang K. 3D printed self-expandable vascular stents from biodegradable shape memory polymer. *Adv Polym Tech* 2018;37(8):3222–8. doi:10.1002/adv.22091.
- [34] Pandey H, Mohol SS, Kandi R. 4D printing of tracheal scaffold using shape-memory polymer composite. *Mater Lett* 2022;329:133238. doi:10.1016/j.matlet.2022.133238.
- [35] Choong YYC, Maleksaeedi S, Eng H, Wei J, Su P-C. 4D printing of high performance shape memory polymer using stereolithography. *Mater Design* 2017;126:219–25. doi:10.1016/j.matdes.2017.04.049.
- [36] Zhang Q, Kuang X, Weng S, et al. Shape-memory balloon structures by pneumatic multi-material 4D printing. *Adv Funct Mater* 2021;31(21):2010872. doi:10.1002/adfm.202010872.
- [37] Chen J, Huang J, Hu Y. 3D printing of biocompatible shape-memory double network hydrogels. *ACS Appl Mater Interfaces* 2021;13(11):12726–34. doi:10.1021/acsami.1c17622.
- [38] Liu H, Wang F, Wu W, Dong X, Sang L. 4D printing of mechanically robust PLA/TPU/Fe3O4 magneto-responsive shape memory polymers for smart structures. *Comp Part B* 2023;248:110382. doi:10.1016/j.compositesb.2022.110382.
- [39] Zhang F, Wen N, Wang L, Bai Y, Leng J. Design of 4D printed shape-changing tracheal stent and remote controlling actuation. *Int J Smart Nano Mater* 2021;12(4):375–89. doi:10.1080/19475411.2021.1974972.
- [40] Zhao W, Zhang F, Leng J, Liu Y. Personalized 4D printing of bioinspired tracheal scaffold concept based on magnetic stimulated shape memory composites. *Compos Sci Technol* 2019;184:107866. doi:10.1016/j.compscitech.2019.107866.
- [41] Simińska-Stanny J, Nizioł M, Szymczyk-Ziółkowska P, et al. 4D printing of patterned multimaterial magnetic hydrogel actuators. *Addit Manuf* 2022;49:102506. doi:10.1016/j.addma.2021.102506.
- [42] Joyee EB, Pan Y. Additive manufacturing of multi-material soft robot for on-demand drug delivery applications. *J Manuf Processes* 2020;56:1178–84. doi:10.1016/j.jmapro.2020.03.059.
- [43] Zhu H, He Y, Wang Y, Zhao Y, Jiang C. Mechanically-guided 4D printing of magneto-responsive soft materials across different length scale. *Adv Intell Syst* 2022;4(3):2100137. doi:10.1002/aisy.202100137.
- [44] Liu C, Wang Z, Wei X, Chen B, Luo Y. 3D printed hydrogel/PCL core/shell fiber scaffolds with NIR-triggered drug release for cancer therapy and wound healing. *Acta Biomater* 2021;131:314–25. doi:10.1016/j.actbio.2021.07.011.
- [45] Kim D, Wu Y, Oh Y-K. On-demand delivery of protein drug from 3D-printed implants. *J Controlled Release* 2022;349:133–42. doi:10.1016/j.jconrel.2022.06.047.
- [46] Wang C, Yue H, Liu J, et al. Advanced reconfigurable scaffolds fabricated by 4D printing for treating critical-size bone defects of irregular shapes. *Biofabrication* 2020;12(4):045025 Aug 18. doi:10.1088/1758-5090/abab5b.
- [47] Luo Y, Lin X, Chen B, Wei X. Cell-laden four-dimensional bioprinting using near-infrared-triggered shape-morphing alginate/polydopamine bioinks. *Biofabrication* 2019;11(4):045019 Sep 13. doi:10.1088/1758-5090/ab39e5.
- [48] Lai J, Ye X, Liu J, et al. 4D printing of highly printable and shape morphing hydrogels composed of alginate and methylcellulose. *Mater Design* 2021;205:109699. doi:10.1016/j.matdes.2021.109699.
- [49] Cao P, Tao L, Gong J, et al. 4D printing of a sodium alginate hydrogel with step-wise shape deformation based on variation of crosslinking density. *ACS Appl Polymer Mater* 2021;3(12):6167–75. doi:10.1021/acsapm.1c01034.
- [50] Han D, Morde RS, Mariani S, et al. 4D printing of a bioinspired microneedle array with backward-facing barbs for enhanced tissue adhesion. *Adv Funct Mater* 2020;30(11):1909197. doi:10.1002/adfm.201909197.
- [51] You D, Chen G, Liu C, et al. 4D Printing of Multi-Responsive Membrane for Accelerated In Vivo Bone Healing Via Remote Regulation of Stem Cell Fate. *Adv Funct Mater* 2021;31(40):2103920. doi:10.1002/adfm.202103920.
- [52] Xin C, Jin D, Hu Y, et al. Environmentally adaptive shape-morphing microrobots for localized cancer cell treatment. *ACS Nano* 2021;15(11):18048–59. doi:10.1021/acsnano.1c06651.
- [53] Ceylan H, Yasa IC, Yasa O, Tabak AF, Giltinan J, Sitti M. 3D-printed biodegradable microswimmer for theranostic cargo delivery and release. *ACS Nano* 2019;13(3):3353–62. doi:10.1021/acsnano.8b09233.
- [54] Magdanz V, Sanchez S, Schmidt OG. Development of a sperm-flagella driven micro-robot. *Adv Mater* 2013;25(45):6581–8. doi:10.1002/adma.201302544.
- [55] Khalid MY, Arif ZU, Noroozi R, Zolfagharian A, Bodaghi M. 4D printing of shape memory polymer composites: a review on fabrication techniques, applications, and future perspectives. *J Manuf Processes* 2022;81:759–97. doi:10.1016/j.jmapro.2022.07.035.
- [56] Dong K, Panahi-Sarmad M, Cui Z, Huang X, Xiao X. Electro-induced shape memory effect of 4D printed auxetic composite using PLA/TPU/CNT filament embedded synergistically with continuous carbon fiber: A theoretical & experimental analysis. *Comp Part B* 2021;220:108994. doi:10.1016/j.compositesb.2021.108994.
- [57] Sarvari R, Keyhanvar P, Agbolaghi S, et al. Shape-memory materials and their clinical applications. *Int J Polymer Mater Polymeric Biomater* 2022;71(5):315–35. doi:10.1080/00914037.2020.1833010.
- [58] Korde JM, Kandasubramanian B. Naturally biomimicked smart shape memory hydrogels for biomedical functions. *Chem Eng J* 2020;379:122430. doi:10.1016/j.cej.2019.122430.
- [59] Hendrikson WJ, Rouwkema J, Clementi F, van Blitterswijk CA, Farè S, Moroni L. Towards 4D printed scaffolds for tissue engineering: exploiting 3D shape memory polymers to deliver time-controlled stimulus on cultured cells. *Biofabrication* 2017;9(3):031001. doi:10.1088/1758-5090/aa8114.
- [60] Zhang C, Cai D, Liao P, et al. 4D Printing of shape-memory polymeric scaffolds for adaptive biomedical implantation. *Acta Biomater* 2021;122:101–10. doi:10.1016/j.actbio.2020.12.042.
- [61] Ramiah P, du Toit LC, Choonara YE, Kondiah PPD, Pillay V. Hydrogel-based bioinks for 3D bioprinting in tissue regeneration. *Review. Front Mater* 2020;7:2020-April-30. doi:10.3389/fmats.2020.00076.
- [62] Shaterabadi Z, Nabiyouni G, Soleymani M. Physics responsible for heating efficiency and self-controlled temperature rise of magnetic nanoparticles in magnetic hyperthermia therapy. *Prog Biophys Mol Biol* 2018;133:9–19. doi:10.1016/j.pbiomolbio.2017.10.001.
- [63] Hu X, Ge Z, Wang X, Jiao N, Tung S, Liu L. Multifunctional thermo-magnetically actuated hybrid soft millirobot based on 4D printing. *Comp Part B* 2022;228:109451. doi:10.1016/j.compositesb.2021.109451.
- [64] Bastola AK, Hossain M. The shape – morphing performance of magnetoactive soft materials. *Mater Design* 2021;211:110172. doi:10.1016/j.matdes.2021.110172.
- [65] Tang J, Yin Q, Shi M, et al. Programmable shape transformation of 3D printed magnetic hydrogel composite for hyperthermia cancer therapy. *Extreme Mechanics Letters*. 2021/07/01/2021;46:101305. doi:https://doi.org/10.1016/j.eml.2021.101305.
- [66] Moreno-Mateos MA, Lopez-Donaire ML, Hossain M, Garcia-Gonzalez D. Effects of soft and hard magnetic particles on the mechanical performance of ultra-soft magnetorheological elastomers. *Smart Mater Struct* 2022;31(6):065018. doi:10.1088/1361-665X/ac6bd3.
- [67] Wang Z, Liu C, Chen B, Luo Y. Magnetically-driven drug and cell on demand release system using 3D printed alginate based hollow fiber scaffolds. *Int J Biol Macromol* Jan 31 2021;168:38–45. doi:10.1016/j.ijbiomac.2020.12.023.
- [68] Tee SY, Win KY, Goh SS, et al. Chapter 1 Introduction to Photothermal Nanomaterials. *Photothermal Nanomaterials. R Soc Chem* 2022:1–32.
- [69] Li J, Zhang W, Ji W, et al. Near infrared photothermal conversion materials: mechanism, preparation, and photothermal cancer therapy applications. *10.1039/D1TB01310F. J Mater Chem B* 2021;9(38):7909–26. doi:10.1039/D1TB01310F.
- [70] Deng Y, Zhang F, Jiang M, Liu Y, Yuan H, Leng J. Programmable 4D printing of photoactive shape memory composite structures. *ACS Appl Mater Interfaces* 2022;14(37):42568–77. doi:10.1021/acsami.2c13982.
- [71] Wei X, Liu C, Wang Z, Luo Y. 3D printed core-shell hydrogel fiber scaffolds with NIR-triggered drug release for localized therapy of breast cancer. *Int J Pharm* Apr 30 2020;580:119219. doi:10.1016/j.ijpharm.2020.119219.
- [72] Biswas MC, Chakraborty S, Bhattacharjee A, Mohammed Z. 4D printing of shape memory materials for textiles: mechanism, mathematical modeling, and challenges. *Adv Funct Mater* 2021;31(19):2100257. doi:10.1002/adfm.202100257.
- [73] Zu S, Wang Z, Zhang S, et al. A bioinspired 4D printed hydrogel capsule for smart controlled drug release. *Mater Today Chem* 2022;24:100789. doi:10.1016/j.mtchem.2022.100789.
- [74] Bozuyuk U, Yasa O, Yasa IC, Ceylan H, Kizilel S, Sitti M. Light-triggered drug release from 3D-printed magnetic chitosan microswimmers. *ACS Nano* 2018;12(9):9617–25. doi:10.1021/acsnano.8b05997.

- [75] Xu H, Medina-Sánchez M, Magdanz V, Schwarz L, Hebenstreit F, Schmidt OG. Sperm-hybrid micromotor for targeted drug delivery. *ACS Nano* 2018;12(1):327–37 2018/01/23. doi:10.1021/acsnano.7b06398.
- [76] Mei Y, Huang G, Solovev AA, et al. Versatile approach for integrative and functionalized tubes by strain engineering of nanomembranes on polymers. *Adv Mater* 2008;20(21):4085–90. doi:10.1002/adma.200801589.
- [77] Findlay-Shirras LJ, Outbih O, Muzyka CN, Galloway K, Hebbard PC, Nashed M. Predictors of residual disease after breast conservation surgery. *Ann Surg Oncol* 2018;25(7):1936–42 2018/07/01. doi:10.1245/s10434-018-6454-1.
- [78] Ock J, Kim T, Lee S, et al. Evaluation of skin cancer resection guide using hyper-realistic in-vitro phantom fabricated by 3D printing. *Sci Rep* 2021;11(1):8935 2021/04/26. doi:10.1038/s41598-021-88287-4.
- [79] Chen Y, Bian L, Zhou H, et al. Usefulness of three-dimensional printing of superior mesenteric vessels in right hemicolectomy cancer surgery. *Sci Rep* 2020;10(1):11660 2020/07/15. doi:10.1038/s41598-020-68578-y.
- [80] Chen Y, Zhang J, Chen Q, et al. Three-dimensional printing technology for localised thoroscopic segmental resection for lung cancer: a quasi-randomised clinical trial. *World J Surg Oncol* 2020;18(1):223 2020/08/24. doi:10.1186/s12957-020-01998-2.
- [81] Tejo-Otero A, Valls-Esteva A, Fenollosa-Artés F, et al. Patient comprehension of oncologic surgical procedures using 3D printed surgical planning prototypes. *Ann 3D Printed Med* 2022;7:100068 2022/08/01/. doi:10.1016/j.stlm.2022.100068.
- [82] Han G, Lee H, Park S, et al. 3D printed drug-eluting bullets for image-guided local chemo-photothermal therapy. *SSRN* 2022. <http://dx.doi.org/10.2139/ssrn.4171677>.
- [83] Cho H, Jammalamadaka U, Tappa K, et al. 3D printing of poloxamer 407 nanogel discs and their applications in adjuvant ovarian cancer therapy. *Mol Pharm* 2019;16(2):552–60 Feb 4. doi:10.1021/acs.molpharmaceut.8b00836.
- [84] Zhang Y, Zhai D, Xu M, Yao Q, Chang J, Wu C. 3D-printed bioceramic scaffolds with a Fe3O4/graphene oxide nanocomposite interface for hyperthermia therapy of bone tumor cells. *J Mater Chem B* 2016;4(17):2874–86. doi:10.1039/C6TB00390G.
- [85] Chen Z, Jin Z, Yang L, et al. A self-expandable C-shaped 3D printing tracheal stent for combinatorial controlled paclitaxel release and tracheal support. *Mater Today Chem* 2022;24:100760 2022/06/01/. doi:10.1016/j.mtchem.2021.100760.
- [86] Huang C-Y, Ju D-T, Chang C-F, Muralidhar Reddy P, Velmurugan BK. A review on the effects of current chemotherapy drugs and natural agents in treating non-small cell lung cancer. *Biomedicine (Taipei)* 2017;7(4) 23-23. doi:10.1051/bmdcn/2017070423.
- [87] Pucci C, Martinelli C, Ciofani G. Innovative approaches for cancer treatment: current perspectives and new challenges. *Ecanermedscience* 2019;13 961-961. doi:10.3332/ecancer.2019.961.
- [88] Yi HG, Choi YJ, Kang KS, et al. A 3D-printed local drug delivery patch for pancreatic cancer growth suppression. *J Control Release Sep* 28 2016;238:231–41. doi:10.1016/j.jconrel.2016.06.015.
- [89] Shi K, Tan DK, Nokhodchi A, Maniruzzaman M. Drop-on-powder 3D printing of tablets with an anti-cancer drug, 5-fluorouracil. *Pharmaceutics* 2019;11(4):150. doi:10.3390/pharmaceutics11040150.
- [90] Dang HP, Shabab T, Shafee A, et al. 3D printed dual macro-, microscale porous network as a tissue engineering scaffold with drug delivering function. *Biofabrication* 2019;11(3):035014 2019/04/26. doi:10.1088/1758-5090/ab14ff.
- [91] Mei Y, He C, Gao C, Zhu P, Lu G, Li H. 3D-printed degradable anti-tumor scaffolds for controllable drug delivery. *Int J Bioprint* 2021;7(4) 418-418. doi:10.18063/ijb.v7i4.418.
- [92] Chen H, Cheng Y, Wang X, et al. 3D printed in vitro tumor tissue model of colorectal cancer. *Theranostics* 2020;10(26):12127–43. doi:10.7150/thno.52450.
- [93] Wang Y, Shi W, Kuss M, et al. 3D bioprinting of breast cancer models for drug resistance study. *ACS Biomaterials Science & Engineering* 2018;4(12):4401–11 2018/12/10. doi:10.1021/acsbomaterials.8b01277.
- [94] Kim MJ, Chi BH, Yoo JJ, Ju YM, Whang YM, Chang IH. Structure establishment of three-dimensional (3D) cell culture printing model for bladder cancer. *PLoS One* 2019;14(10):e0223689. doi:10.1371/journal.pone.0223689.
- [95] Wang Y, Sun L, Mei Z, et al. 3D printed biodegradable implants as an individualized drug delivery system for local chemotherapy of osteosarcoma. *Mater Design* 2020;186:108336 2020/01/15/. doi:10.1016/j.matdes.2019.108336.
- [96] Shi X, Cheng Y, Wang J, et al. 3D printed intelligent scaffold prevents recurrence and distal metastasis of breast cancer. *Theranostics* 2020;10(23):10652–64. doi:10.7150/thno.47933.
- [97] Gellci K, Mehrmohammadi M. Photothermal therapy. In: Schwab M, editor. *Encyclopedia of cancer*. Berlin Heidelberg: Springer; 2014. p. 1–5.
- [98] Guillemain PC, Dipasquale G, Uiterwijk JW, et al. Magnetic resonance-guided ultrasound hyperthermia for prostate cancer radiotherapy: an immobilization device embedding the ultrasound applicator. *J 3D Print Med* 2022;6(2):13. doi:10.2217/3dp-2021-0024.
- [99] Mukai Y, Li S, Suh M. 3D-printed thermoplastic polyurethane for wearable breast hyperthermia. *Fashion Textiles* 2021;8(1):24 2021/05/15. doi:10.1186/s40691-021-00248-7.
- [100] Roeth AA, Garretson I, Beltz M, et al. 3D-printed replica and porcine explants for pre-clinical optimization of endoscopic tumor treatment by magnetic targeting. *Cancers (Basel)* Nov 1 2021;13(21). doi:10.3390/cancers13215496.
- [101] He C, Dong C, Yu L, Chen Y, Hao Y. Ultrathin 2D inorganic ancient pigment decorated 3d-printing scaffold enables photonic hyperthermia of osteosarcoma in NIR-II biowindow and concurrently augments bone regeneration. *Adv Sci* 2021;8(19):2101739. doi:10.1002/advs.202101739.
- [102] Nguyen VD, Nguyen KT, Zheng S, et al. A magnetically-controlled 3D-printed helical microrobot for application in photothermal treatment of cancer cells. 2022:1-5.
- [103] Paunović N, Marbach J, Bao Y, et al. Digital light 3D printed bioresorbable and NIR-responsive devices with photothermal and shape-memory functions. *Adv Sci* 2022;9(27):2200907. doi:10.1002/advs.202200907.
- [104] Chu C-H, Liu R, Ozkaya-Ahmadov T, et al. Hybrid negative enrichment of circulating tumor cells from whole blood in a 3D-printed monolithic device. *J Lab Chip* 2019;19(20):3427–37. doi:10.1039/C9LC00575G.
- [105] Germain N, Dhayer M, Dekiouk S, Marchetti P. Current advances in 3D bioprinting for cancer modeling and personalized medicine. *Int J Mol Sci* 2022;23(7):3432.
- [106] Kang Y, Datta P, Shanmughapriya S, Ozbolat IT. 3D bioprinting of tumor models for cancer research. *ACS Appl Bio Mater* 2020;3(9):5552–73 2020/09/21. doi:10.1021/acsbm.0c00791.
- [107] Naniz MA, Askari M, Zolfagharian A, Bodaghi M. 6 - 4D bioprinting: fabrication approaches and biomedical applications. In: Bodaghi M, Zolfagharian A, editors. *Smart Materials in Additive Manufacturing*. Elsevier; 2022. p. 193–229.
- [108] Chadwick M, Yang C, Liu L, et al. Rapid processing and drug evaluation in glioblastoma patient-derived organoid models with 4D bioprinted arrays. *iScience* 2020;23(8):101365 Aug 21. doi:10.1016/j.isci.2020.101365.
- [109] Yang C, Luo J, Polunas M, et al. 4D-printed transformable tube array for high-throughput 3D cell culture and histology. *Adv Mater* 2020;32(40):2004285. doi:10.1002/adma.202004285.
- [110] Pugliese R, Regondi S. Artificial intelligence-empowered 3D and 4D printing technologies toward smarter biomedical materials and approaches. *Polymers* 2022;14(14):2794.
- [111] Lin Z, Chou W-C, Cheng Y-H, He C, Monteiro-Riviere NA, Riviere JE. Predicting nanoparticle delivery to tumors using machine learning and artificial intelligence approaches. *Int J Nanomed* 2022;17:15. doi:10.2147/IJN.S344208.